Development of nanocarriers for the treatment of Alzheimer' s disease

Telma Sofia Mendes Ferreira

UMinho | 2021

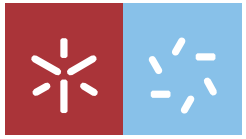

Universidade do Minho
Escola de Ciências

Telma Sofia Mendes Ferreira

Development of nanocarriers for the treatment of Alzheimer's disease

agosto de 2021

Universidade do Minho
Escola de Ciências

Telma Sofia Mendes Ferreira

Development of nanocarriers for the treatment of Alzheimer's disease

Dissertação de Mestrado
Mestrado em Bioquímica Aplicada
Biomedicina

Trabalho efetuado sob a orientação de
Professora Doutora Andreia Ferreira de Castro Gomes

agosto de 2021

Acknowledgments/Agradecimentos

Em primeiro lugar, gostaria de agradecer à Professora Doutora Andreia Gomes, por toda a ajuda, suporte e compreensão. Num ano tão atípico como este foi, agradeço toda a dedicação e energia para a elaboração desta tese, até ao último momento. Um especial Obrigada.

Agradeço ao Mário, por estar sempre disponível a toda a hora, mesmo com todo o seu trabalho para fazer. Agradeço por estar sempre lá, por toda a paciência, por nunca desistir de me ajudar mesmo quando o tempo era escasso, por toda a companhia ao longo deste tempo, por me ajudar a crescer no laboratório.

A todos os que partilharam comigo o laboratório, agradeço por me ajudarem a perceber toda a dinâmica laboratorial e a tornar-me mais autónoma.

À Carina, Flávia e Laura, as pessoas com quem mais convivi durante este ano, agradeço por todo o otimismo e apoio, por me motivarem mesmo quando nem eu sabia que precisava de ser motivada, por toda a companhia. Agradeço pelo ano fantástico que me proporcionaram.

Ao Berto, obrigada pelos momentos de descontração, que foram fundamentais para ter força para voltar ao trabalho o mais focada possível.

Agradeço ao Diogo, meu namorado, por estar comigo no melhor e no absolutamente pior. Por nunca me deixar desistir, mesmo quando parecia não haver nenhuma outra saída. Pela companhia em absolutamente todos os momentos, obrigada.

Agradeço aos meus Pais, sem eles nada disto seria possível. Pelo suporte e apoio, pelo incentivo e por todas as palavras de carinho e amor, por estarem sempre prontos para me ajudar, obrigada.

À minha irmã, agradeço por sem saber, com a sua inocência, conseguir inspirar-me e motivar-me a não desistir, a lutar, a tentar sempre.

Agradeço à minha avó, que tem sempre uma palavra de conforto e de carinho para dizer, que faz o que for preciso para me ver feliz.

Por fim, agradeço a quem já não está presente, mas que foram sem dúvida o meu maior incentivo e a minha maior força para acabar este trabalho. Obrigada, avô e avó.

STATEMENT OF INTEGRITY

I hereby declare having conducted this academic work with integrity. I confirm that I have not used plagiarism or any form of undue use of information or falsification of results along the process leading to its elaboration.

I further declare that I have fully acknowledged the Code of Ethical Conduct of the University of Minho.

Resumo

Desenvolvimento de nanotransportadores para o tratamento da doença de Alzheimer

O cérebro é o órgão mais complexo do corpo humano, o mais difícil de entender e o mais bem protegido do nosso corpo. A proteção gerada à sua volta é tanto uma vantagem como uma desvantagem e a maior dificuldade no desenvolvimento de terapêuticas para patologias tão severas, incapacitantes e debilitantes, como é o caso da Doença de Alzheimer. A Aβ-amilóide, um péptido, devido a uma alteração no metabolismo é progressivamente produzido e depositado, levando à formação das placas senis. Além disso, como a Aβ-amilóide é responsável por regular determinadas vias de sinalização, a sua desregulação provoca uma hiperfosforilação da proteína TAU. Estas duas condições são os principais pilares onde a investigação atual da doença de Alzheimer assenta e procura entender e resolver.

O encapsulamento em lipossomas, de curcumina e siRNA, duas moléculas com potencial terapêutico, e a sua posterior libertação no cérebro, são uma maneira de evitar a progressão desta doença, uma vez que se descobriu que a curcumina tem afinidade para os agregados de Aβ-amilóide e capacidade neuroprotetora, e através de siRNA exógeno pretende-se obter o silenciamento de genes envolvidos na patologia. O encapsulamento de ambas as substâncias foi alcançado, conseguindo-se manter as características ideias de tamanho dos lipossomas para que consigam atravessar a barreira hematoencefálica. Foi necessário avaliar se estas formulações de lipossomas não seriam tóxicas para as células e, portanto, foram estudadas em duas linhas celulares: L929, fibroblastos de ratinho, e SH-SY5Y, neuroblastoma humano. Verificou-se que as formulações alcançadas não apresentam toxicidade significativa. O passo seguinte seria testar as formulações *in vivo*, em embriões de peixe-zebra.

Palavras-chave: acetilcolinesterase, Alzheimer, citotoxicidade, lipossomas

Abstract

Development of nanocarriers for the treatment of Alzheimer's disease

The brain is the most complex, the most difficult to understand and the best protected organ in the human body. The protection generated around it is both an advantage and a disadvantage and the greatest difficulty in developing therapies for such severe, disabling and debilitating pathologies as Alzheimer's Disease. Amyloid-β, a peptid, due to na alteration in metabolism is progressively produced and deposited leading to the formation of senile plaques. Furthermore, as amyloid-β is responsible for regulating certain signaling pathways, its dysregulation causes a hyperphosphorylation of the TAU protein. These two conditions are known as the hallmarks of Alzheimer's Disease and it is where the current research into Alzheimer's Disease rests and seeks to understand and resolve.

Encapsulation in liposomes of curcumin and siRNA, two molecules with therapeutic potential, and their subsequent release in the brain is a way to prevent the progression of this disease, as curcumin has been found to have an affinity for amyloid-β aggregates and siRNA is one of the most used therapies for gene-silencing. Encapsulation of both substances was achieved and maintaining the ideal size characteristics of the liposomes so that they can cross the blood-brain barrier (BBB). It was necessary to assess whether these liposomes formulations would not be toxic to the cells therefore they were studied in two cell lines: L929, mouse fibroblasts, and SH-SY5Y, human neuroblastoma. It was found that the formulations do not present significant toxicity. The next step would be to test the formulations *in vivo*, on zebrafish embryos. In this study we also assessed the potential neuroprotector effect of the liposomes through the evaluation of the acetylcholinesterase activity behavior.

Keywords: acetylcholinesterase, Alzheimer, cytotoxicity, liposomes

Table of Contents

Abbreviations

AChE	Acetylcholinesterase
AD	Alzheimer's disease
AO	Acridine Orange
APP	Amyloid Precursor Protein
ATCh	Acetylthiocholine
BBB	Blood-brain barrier
CNS	Central nervous system
DLS	Dynamic Light Scattering
DMEM	Dulbecco's Modified Eagle's Medium
DMSO	Dimethyl Sulfoxide
DODAP	Dimethylammonium-propane
DPPC	Dipalmitoylphosphatidylcholine
DTNB	5,5′-dithiobis-(2-nitrobenzoic acid)
ELS	Electrophoretic Light Scattering
FBS	Fetal Bovine Serum
HEPES	4-(2-hydroxyethyl)-1-piperazineethanesulfonic acid
KA	Kainic acid
MAPT	Microtubule-associated protein TAU
LUV	Large unilamellar vesicles
miRNAs	MicroRNAs
MK-801	Dizocilpine
MLV	Multilamellar vesicles
MPTP	1-methyl-4-phenyl-1,2,3,6-tetrahydropyridine
MTT	Methyl Tetrazolium
NFTs	Neurofibrillary tangles
NGF	Nerve Growth Factor
NMDA	N-methyl-D-aspartate
NO	Nitric oxide
PDI	Polydispersity
PEG	Polyethylene glycol
PI	Propidium Iodide

PTZ	Pentylenetetrazol
qPCR	Quantitative polymerase chain reaction
RNAi	RNA interference
ROS	Reactive oxygen species
siRNA	Small interfering RNA
SUV	Small unilamellar vesicles
***t*BHP**	*tert*-butyl hydroperoxide

Figure Index

Table Index

1. Introduction

1.1. NEURODEGENERATIVE DISORDERS

The brain is known to be the most complex organ in the human body and also the most important since it controls the rest of the human body. Given its complexity, it is understandable that the mechanisms of dysfunction and their functioning are not yet well understood, despite the enormous scientific advances of the last decade [1].

Psychiatric disorders are multifaceted, involving the interaction of multiple genetic and environmental factors, which affect both brain and behavioral processes, either at the level of thoughts, feelings and mood [2] or at the level of social interactions. Some of the diseases that affect the ability to socially interact are schizophrenia, depression and the neurodegenerative disorders, being the most well-known of this group the Huntington's, Parkinson's and Alzheimer's diseases [3]. The neurodegenerative disorders affect the brain in a way that leads to the death of neurons, meaning that there is a loss at the level of the brain structure. The pathologic characteristic that is common in neurodegenerative disorders and that implies an important molecular mechanism is the presence of the abnormal amyloid protein [4]. Amyloids are a group of proteins that clump together into amyloid fibrils and vary according to the neurodegenerative disease in question. In Alzheimer's disease (AD) are present the amyloids–β (Aβ), in Parkinson's disease the α-synucleins and in Huntington's disease the huntigtines [5].

The increase in population longevity was accompanied by an increasing need to find more effective treatments. More specifically, the need for preventive treatments since the ones who exist only relieve symptoms, that is, are just palliative treatments. A very prominent example is dementia associated with AD, which represents a burden on patients, family and the economy [6], being one of the greatest forms of dependency, disability and mortality [7].

1.2. ALZHEIMER'S DISEASE

AD is a neurodegenerative disease and the most prevalent subtype of dementia, a generic term used to describe the progressive loss of the cognitive function, resulting in the death or lack of normal functioning of the neurons (Figure 1). This chronic loss of neurons, particularly cholinergic neurons, and therefore synapses in the cerebral cortex lead to a series of consequences, known to be the characteristics of AD, such as memory and orientation loss, cognitive deprivation and death [5], [8], [9]. It is estimated that approximately 47 million people worldwide suffer from this disease, with AD recognized by the World Health Organization as a global public health priority [10], [7].

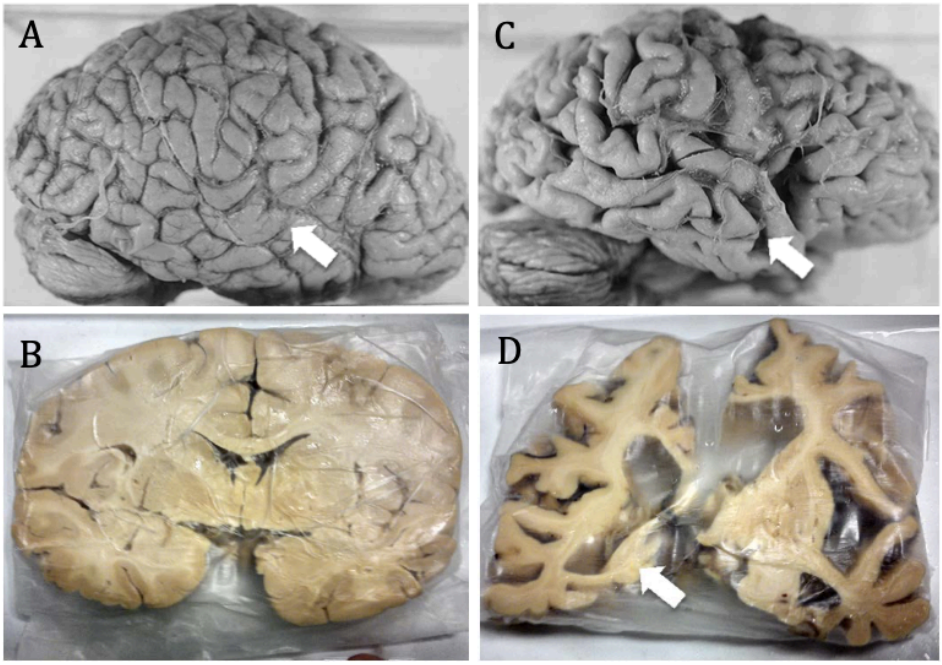

Figure 1. The comparison between a normal brain (A and B) and a brain with Alzheimer's (C and D) [17].

The two hallmark pathologies for the diagnosis of AD are the extraneuronal accumulation of amyloid-β plaques in the nervous system and a parallel intraneuronal aggregation of neurofibrillary tangles (NFTs), formed by hyperphosphorylation of the Tau protein in the brain [11], [12]. A critical step in the development of the disease is the formation of senile plaques – extracellular deposits of amyloid-β in the gray matter of the brain – that compress the fibrils of the amyloid peptide [13].

An enzyme that is of vital importance for the study of AD is acetylcholinesterase. Acetylcholinesterase (AChE) is an enzyme that stops the sign between a nerve cell and a muscle cell. This enzyme breaks the neurotransmitter acetylcholine in acetic acid and choline which stops the signal and prevents muscle paralysis induced by the acetylcholine. Poisons and toxins used to be administrated aiming this enzyme however nowadays it is being studied the partial block of acetylcholinesterase as an attempt to revert symptoms of AD. People who suffer from AD are known to lose many nerve cells so the aim is to by partially blocking this enzyme's activity, increase the neurotransmitter levels therefore strengthening the remaining nerve signals [14], [15], because its inhibition prolongs the duration and intensity of acetylcholine at synaptic terminals, improving cholinergic transmission (Figure 2) [16].

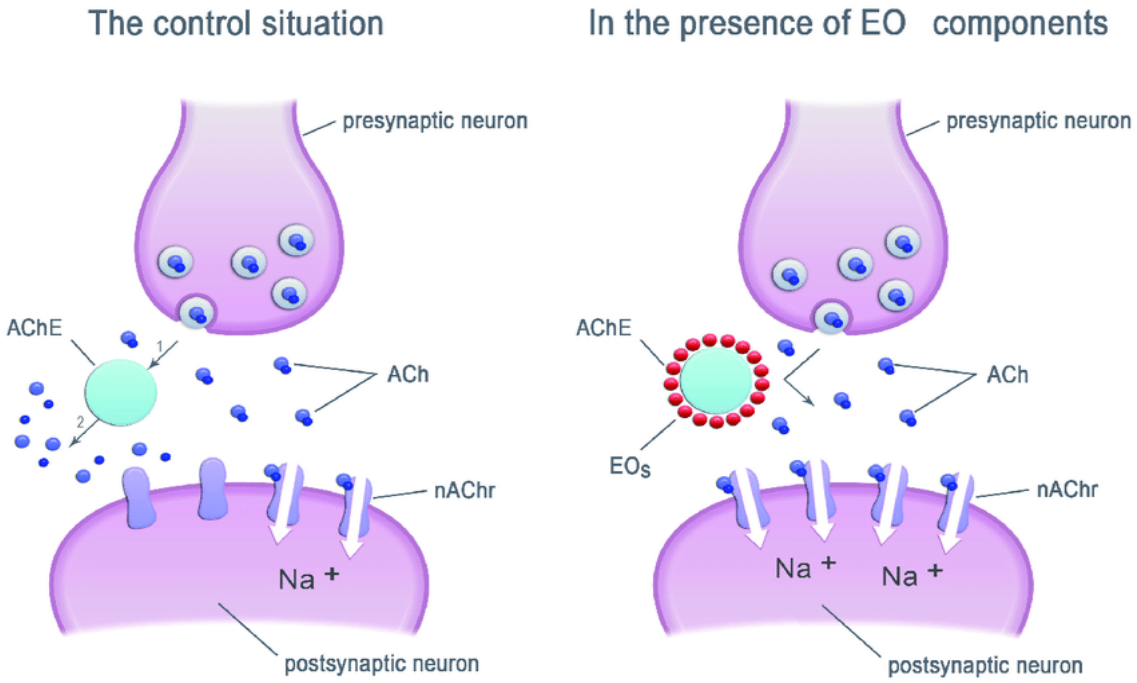

Figure 2. Mode of action of acetylcholinesterase enzyme [16].

1.2.1. Accumulation of amyloid-β plaques

Amyloid Precursor Protein (APP), a glycoprotein, is an integral membrane protein that is expressed in the central nervous system, in many tissues, especially in the synapses of neurons. Its physiological function is not fully disclosed but it is known to play an important role in brain development, memory and synaptic plasticity [17]–[19]. The proteolytic cleavage of the APP results in a 38-43 amino acid peptide, the amyloid-β peptide, that is the main component of senile plaques. In AD, an alteration in APP metabolism is associated with a progressive increase in the

production and abnormal deposition of amyloid-β [17]. This accumulation and posterior aggregation of amyloid-β in the cerebral extracellular space leads to the formation of the amyloid plaques, a pathological hallmark of AD. Although in some individuals with extensive amyloid-β deposits no signs of dementia are detected, there is still a strong association between the amyloid plaques and AD [19].

Due to the aggregates of amyloid-β an inflammatory response is triggered leading to the activation of several pathological signaling pathways, that result in neurodegeneration [20], [21]. One of this pathways is the oxidative stress pathway, defined by a disturbance in the balance between reactive oxygen species (ROS) and antioxidant defenses, which results in an alteration at the level of lipids, proteins and nucleic acids as well as in cell death [17]. An accumulation of free radicals, such as nitric oxide (NO), is the main reason to cause oxidative stress in AD [20]. Normally, under physiological conditions, the amyloid-β is responsible for regulating the release of NO, whose levels increase under conditions of inflammation. Hence, in AD**,** the synthesis of NO is promoted and the increase of these levels could lead to the formation of NFTs leading to an increase of tau phosphorylation, which is an hallmark of AD [17], [21].

1.2.2. Hyperphosphorylation of TAU and NFTs

Due to the aggregation of abnormally phosphorylated TAU protein, AD integrates a group of disease denominated “tauopathies” [22].This microtubule-associated is a phosphoprotein that can be found in many tissues [23], but is most abundantly expressed and commonly found in the axons of central nervous system neurons [12], being involved in the cycle of association-dissociation of microtubules [22], [24]. TAU protein is the main component of NFTs, intracellular fibrillar structures, that are fundamental neuropathological hallmarks of AD [25]. NFTs are not specific of AD, as they can be found in almost every category of brain disease, and the number as well as the localization of NFTs are known to be correlated with the level of dementia [24], [26]. The hyperphosphorylation of TAU prevents it to bind to microtubules, that therefore become unstable and begin to disintegrate, which compromises the axonal transport (Figure 3) [27].

The incapacity of hyperphosphorylated TAU of binding tubulin is due to its self-aggregation into insoluble inclusions, the NFTs. So, NFTs are nothing less than deposits of TAU protein, in an insoluble misfolded and hyperphosphorylated state, in the neuronal cytoplasm and that's why the appearance of tangles is correlated with neuronal loss [27], [25].

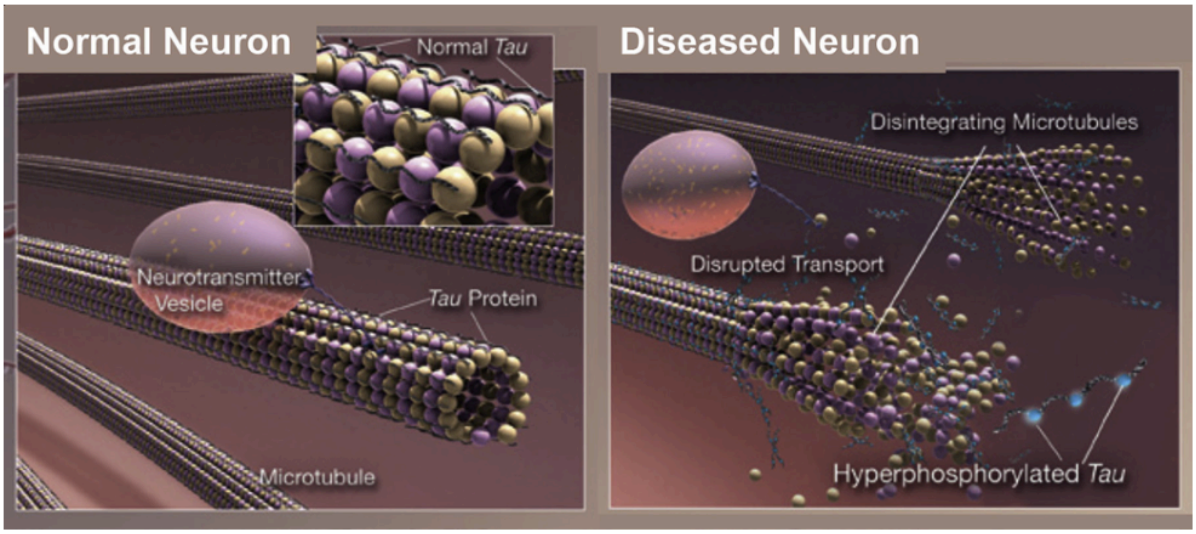

Figure 3. The behavior of TAU protein in a healthy brain (left) versus in a diseased brain (right) [27].

MAPT is the gene responsible for encoding protein TAU. Specific mutations in this gene can trigger frontotemporal dementia which is indicative that tauopathy plays a causal role in neurodegeneration, even though the exact mechanism is not clear. Thus, a clear insight on the mechanism of tauopathy induction and consequent neurodegeneration may represent an important breakthrough in tau-targeting therapeutics [28].

1.2.3. Promising therapeutics

Most dementias, AD included, are, for now, untreatable. As it is a progressive disease, all that can be done is treat the symptoms. In fact, a significant number of laboratories investigate and work to achieve a treatment for this disease, a burden for both the patient and the caregiver [27]. There are several attempts at a cure, targeting either the senile plaques or the TAU protein. A few therapeutic approaches are the development of a vaccine that targets and destroys the amyloid-β; the delivery of Nerve Growth Factor (NGF), in order to prevent cholinergic neuronal death [27]; microRNAs (miRNAs), to try and regulate APP expression [18]; the inhibition of pathological TAU aggregation or the modulation of TAU phosphorylation [12], among others. Those approaches can be performed either through direct injection of drugs or immunotherapy, among

others. There are also recent studies concerning nanodelivery of drugs, via nanoparticles [13], [18]. However, what makes AD an hard disease to cure is the blood-brain barrier (BBB), that makes the task of delivering drugs to the brain a difficult accomplishment [27].

1.2.4. Blood-Brain Barrier

The central nervous system (CNS) is protected by a variety of barriers, to prevent the entry of unwanted compounds. The blood-brain barrier (BBB) is a highly selective barrier, constituted by blood vessels built by a set of specialized endothelial cells, astrocytes, pericytes and neuronal terminations [28]. It reduces the entry of molecules into the brain tissue, protects against harmful external agents and helps maintain the microenvironment of the brain stable, all of this while providing with the necessary supplying nutrients, in order to maintain the homeostasis of the brain, since neurons are very sensitive cells even to the smallest changes [28], [29]. This impediment is due to the tight junctions that are formed between adjacent endothelial cells [29]. The downside of this barrier is that it hinders the entry of therapeutic compounds in the brain. Although the majority of molecules cannot get through, it is already known that some small molecules, with specific molecular weight, lipophilicity and charge, are able to diffuse from the blood to the CNS [28], [30], which is a good starting point to subsequent studies.

1.3. NANOSYSTEMS

Nanotechnology has become one of the most prominent technologies in science. It is described by the ability to measure, see, manipulate, manufacture and apply structures by controlling size and shape, on an atomic or molecular scale [31], [32]. Richard Feynman, an American physicist, one of the pioneers of quantum electrodynamics, was the first to hypothesize the possibility of manipulating and maneuvering things at an atomic level, still in the 50s [33]. This field involves a wide variety of areas, such as biology, chemistry and physics of objects at the nanoscale [34]. Nanosystems exist everywhere, from computers, programming devices and sensors to medical devices, gene delivery and theragnostic, being used in several areas, such as in the cosmetic, food, pharmaceutical and textile industries, as well as in medicine. Throughout the years, nanosystems for controlled delivery of active substances became indispensable in drug delivery, in diagnosis and detection, in therapy, in cosmetics and in medical applications [35], offering a series of benefits such as cancer imaging and diagnosis, real-time assessment of efficacy of a treatment, substances capable of detecting molecular alterations, alternative paths for insulin delivery, detection of mutations and neurological diseases [36].

Nanoparticles are discrete particles, approximately between 1 and 100 nm [37], and possess certain manipulable characteristics, such as the material from which they are made, their size, shape, electrical charge, optical properties and, in addition, they can be modified through the combination of reactive functional groups and charges. These particles can be synthesized by several methods, including chemical and physical. The production of these particles is made with a wide variety of materials, such as lipids, polymers, macromolecules, silica, metals, and proteins. Besides that, living organisms, such as plants, fungi and bacteria can also be used for the synthesis of nanoparticles [38], [34], [39]. An example of nanoparticles are the exosome-like nanoparticles, that can be extracted from plants, such as grapes, lemon tree, carrots or ginger; can be extracted from animal cells or can be merged with liposomes [40].

The design of nanoparticles, among many other reasons, is due to the growing need to create new techniques for preventing and fighting diseases involved in human health, having been developed in order to be selectively attracted to the affected cells and tissues, promoting its regeneration or programed death thus allowing the treatment of the patient [41], [42].

The area-volume ratio of these particles means that they exhibit a series of properties that allow them to be used for a variety of function and areas, such as in health, food, chemistry, the cosmetic and pharmaceutical industry and agriculture, since the volume affects the area of the

nanoparticles, that is, a bigger volume displays a bigger size [43]. They are also applicable in several research areas, including drug delivery, since they may have the ability to prevent the immune response and cross impermeable membranes in diagnoses and treatments [44], the latter being due especially to their size, shape and thermal characteristics and unique optics [34], [44]. These properties are what determines the ability of nanoparticles to interact with cells or to affect biochemical reactions [37].

The morphological parameters of the nanoparticles, such as size, charge and selectivity for the target to which they are directed, can be modulated by varying the concentration of chemicals and the reaction conditions [45]. They affect absorption, distribution, metabolism and excretion, which are essential processes in modulating the *in vivo* activity of the transported bioactive (Figure 4) [46].

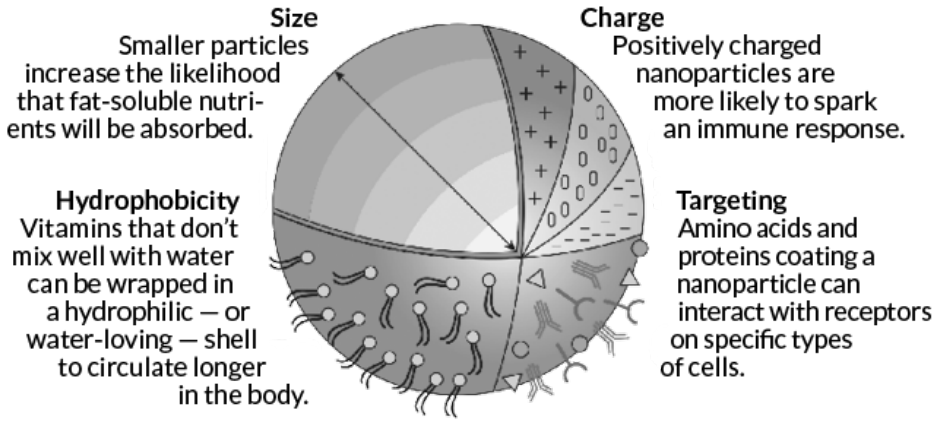

Figure 4. Physicochemical properties that directly affect interactions with cells, tissues and organs (adapted from [47]).

1.3.1. Nanocarriers used for AD treatment

Quite broadly, nanoparticles can be divided into inorganic and organic (Figure 5) [47], [40]. Organic nanoparticles include liposomes, micelles and solid lipid nanoparticles. Inorganic nanoparticles include gold, silver, silica and polymeric nanoparticles as well as carbon, nickel and magnetic nanotubes. The possible applications of nanoparticles vary according to its composition [48], [32], [40].

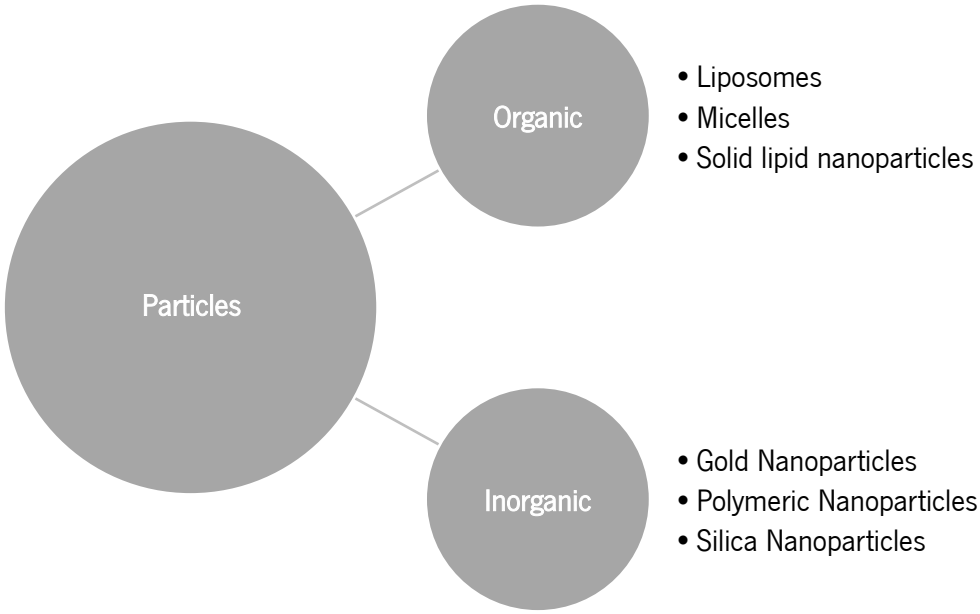

Figure 5. Distinction between organic (liposomes, micelles and solid lipid nanoparticles) and inorganic (gold nanoparticles, polymeric nanoparticles and silica nanoparticles) particles.

All these particles mentioned above have been studied and some of them are known to be able to cross the BBB and are the main kind of particles used in the study of AD. The organic nanoparticles show some advantages over the others because they are highly biocompatible and biodegradable, making them suitable for a wide spectrum of biomedical applications [48]. Although the nanoparticles being interesting for drug delivery, they face a big challenge since some studies show that the accumulation of the particles in organs such as the liver and the kidney can be very harmful so the main concern in the making of nanoparticles is to produce non-cytotoxic nanoparticles. At the moment, liposomes are one of the most used in therapy since they are able to overcome the previous concern [40] and also liposomes possess a characteristic of being easy to modify its surface in order to being able to efficiently target the local of interest.

1.3.2. Liposomes

The aim of using liposomes as drug delivery systems is to reduce the toxic side effects of the free drugs accumulation in organs such as kidney, liver and heart and also to enhance the target of specific tissues. Liposomes are biodegradable and biocompatible, therefore making no harm to the human body. Depending on their diameter, liposomes can be classified into small unilamellar vesicles (SUV), large unilamellar vesicles (LUV) and multilamellar vesicles (MLV) [49].

The potential of liposomes as drug delivery systems was recognized after the verification of their capacity to form a phospholipid bilayer whose structure allows the storage of biologically

active materials. This bilayer is spontaneously formed by phospholipids dispersed in an aqueous medium, through self-organization. Liposomes possess the unique ability of carrying incorporated substances since they can insert the hydrophobic molecules within the bilayer while the hydrophilic molecules are stored in its aqueous interior.

In addition to being able to encapsulate substances and to carry and delivery them, it is also possible to come across different formulations [50]. For the liposomes to be able to cross the BBB and, before that, to move in the serum without being identified and eliminated, some of the properties that characterize liposomes, such as its charge, lipid composition, size and surface modification, can be manipulated and optimized [51], [52]. And even though studies show that liposomes are capable of crossing the BBB, a new challenge appears after that: the microglia cells, known as the brain resident immune cells, that are responsible for recognizing and targeting foreign substances and to posterior eliminate them. So that is another thing to have in account when thinking about the delivery of a drug [48], [53].

1.3.2.1. Exosome-like nanoparticles

Exosomes are naturally occurring vesicles that transport proteins, nucleic acids, and other molecules (Figure 6) [54].

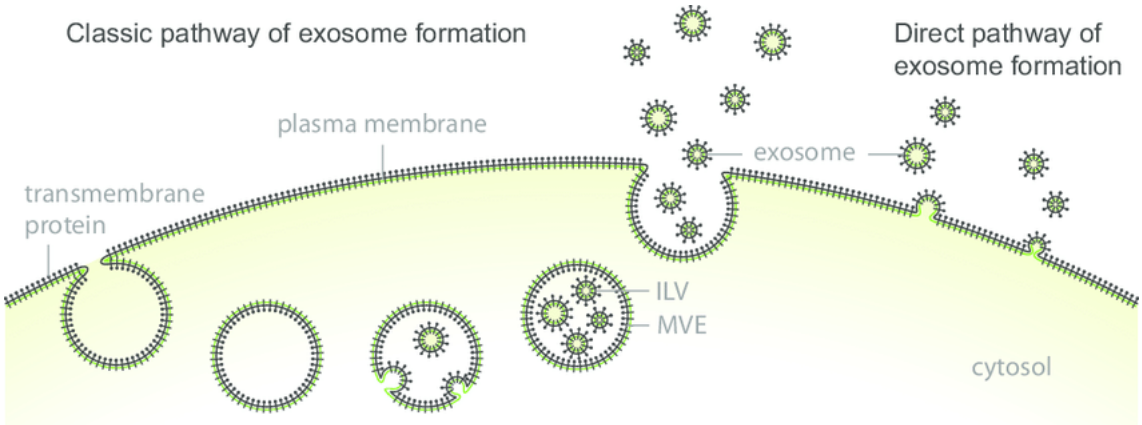

Figure 6. Classic pathway of exosome formation [54].

Exosome-like nanoparticles are formulated with similar properties to exosomes. They can facilitate transport across the blood-brain barrier and, also, lipids present in exosomes do not show toxicity, as they are from human cells. These systems are capable of encapsulating curcumin and siRNA, which are molecules of interest for the treatment of AD [40]. Exosomes provide several

advantages, such as they are occurred naturally in the human body, so they are stable under physiological conditions; are less toxic in comparison with other nanocarriers; they enhance the delivery efficiency because it is their function to deliver cargo to specific targets; and lastly, exosomes have the ability to cross the blood-brain barrier. On the other side, the use of exosomes lacks a standard method for its isolation and purification, and also it is not well known how the different cell types affect the exosomes derived from other cell types [55].

After the formulations of liposomes, it is essential to purify them so that the encapsulated fraction can be separated from the free fraction. There are a wide range of possibilities for purifying liposomes. Since all methods have their advantages and disadvantages, the chosen method depends on the characteristics of the liposomes to be purified. According to the literature, the most used methods are dialysis, size separation chromatography and centrifugation (Table 1) [56], [57].

Table 1. Description of the different techniques that can be used in liposome's purification.

Method	Material	Description
Dialysis	Semipermeable membrane	Widely used technique that consists of separating the free drugs from the liposomes by using a semipermeable membrane, whose pores allow only the smallest molecules, the free drugs, to pass. Despite the advantages, such as low cost and large amount of sample that can be processed at the same time, it is a method that at room temperature can take up to 24H to finish, which is a long time [56], [57].
Size Separation Chromatography	Molecular Exclusion Column	A molecular exclusion column consisting of a gel is used. The most used gels are Sepharose and Sephadex. The choice of the gel is related to the characteristics of the particles. The basic principle of this method is the separation based on the molecular weight of particles. The free drugs, because they have less molecular weight, enter the pores of the gel more easily, being retained for longer. In this way the liposomes are eluted more quickly, being the first to be caught [58].

Centrifugation	Centrifuge	There are several types of centrifugations, such as micro centrifugation or ultracentrifugation, but they all involve the application of centrifugal forces. Thus, while the free drugs pass through the filter together with the supernatant, the liposomes remain at the bottom of the centrifuge tube. However, this method requires high rotation speeds that can result in the aggregation of particles, the release of the encapsulated drug or the rupture of the liposomal membrane [57].

For a better stabilization and longer circulation time, there are several changes that can be made in lipid composition, such as maintaining a size equal to 100 nm. Also, the addition of polyethylene glycol to the formulations delays the elimination process [59], [60].

1.3.2.2. Curcumin

Curcumin is a natural polyphenolic compound with a yellow coloration, extracted from *Curcuma longa*, that is relatively stable at high temperatures however it is extremely sensitive to light. Curcumin has been very studied over the years due to its therapeutic properties such as antibacterial, anti-inflammatory, anti-neoplastic and antioxidant properties [61]. As shown in various studies in the last years, curcumin has a high affinity at the level of amyloid-β peptides, having an important role in preventing the formation of amyloid-β plaques and in disrupting the already existent aggregates. This makes curcumin a substance of particular interest in the study of AD [52], [53], [62]. In addition, curcumin has been reported to display an inhibitory effect acetylcholinesterase, thus an assay to assess the activity of acetylcholinesterase in the presence of curcumin is an important tool to determine curcumin's bioactivity [64].

Curcumin alone has the disadvantage of being relatively unstable and of poor bioavailability due to its hydrophobic behavior [52], [61]. Therefore, its properties can be changed when it is in contact with slightly alterations of the surrounding environment, such as, for example, low/high pH or aqueous conditions [61]. So, in order to be delivered to the proper site of action and still maintain its properties, curcumin can be transported by liposomes within the phospholipid bilayer, which increases the efficiency of the therapy [65].

1.3.2.3. Small Interfering RNA (siRNA)

Therapies using gene-silencing by RNA interference (RNAi) have been increasingly studied. This therapy has been studied in several fields, such as in cancer, neurodegenerative diseases, infections and inflammations, since it has become known that many of these diseases are caused by the overexpression of one or more genes. There are three main categories of gene-silencing molecules: derivatives of antisense oligonucleotides, ribozymes and deoxyribozymes; small interfering RNA (siRNA) molecules [66].

siRNA is a small molecule that has around 21 to 23 nucleotides [67] and is one of the most used in gene-silencing, having the potential to be used as a therapy in the treatment of AD, by silencing specific genes associated with the disease [67], [68]. However, this technique faces great challenges: first, the large and hydrophilic structure of siRNA prevents it from being delivered intracellularly; secondly, the molecules are not stable in the serum and are subject to degradation and lastly, the siRNA half-life time without protection is very short [66]. Therefore, the siRNA carrier must protect it from degradation during transport, make sure it is delivered to the target cells and release the siRNA intracellularly. To overcome these problems, it can be encapsulated within liposomes and this way be safely delivered to the site of action without suffering any alterations and maintaining its properties [67], [68].

One way to avoid interactions with blood or other extracellular elements may be to use PEG in the formulation of liposomes [69], [70]. To facilitate the uptake by target cells, what is described in the literature is that using a cationic lipid leads to the formation of a complex in which RNA is surrounded by negative charges [70], [71]. This complex will have the facility to fuse with the negative-charged surface of the cells, allowing siRNA to be released intracellularly [72]. Liposomes without DODAP, for example, are not able to encapsulate siRNA because of its negative charge. Since siRNA is negatively charged, the positive charge of DODAP neutralizes the negative charge of siRNA. Their electrostatic interaction leads to the formation of lipoplexes – a nanocomplex with the material genetic entrapped. These interactions protect RNA from degradation and enable a higher capacity of transfection activity [70], [73].

For the quantification of siRNA several methods are described in the literature. The most used are qPCR, radiolabeled siRNA and fluorescence-labeled siRNA (Table 2) [74].

Table 2. Advantages and disadvantages of some of the siRNA quantification methods [74].

Method	Advantages	Disadvantages
qPCR	- Allows the quantification of specific nucleic acid sequences through the cyclic amplification of the template. - High degree of accuracy.	- Requires quite expensive material. - Extensive optimization.
Radiolabeled siRNA	- Highly sensitive. - Able to detect very low siRNA values.	- Requires laboratory license, qualified personnel and special waste management.
Fluorescence-labeled siRNA	- Commercially available. - Easy to detect and handle.	- Due to the different catabolism rates of the label and siRNA it can be misleading.

1.4. EXPERIMENTAL MODELS

In Figure 7, it is described several experimental models used in research [75].

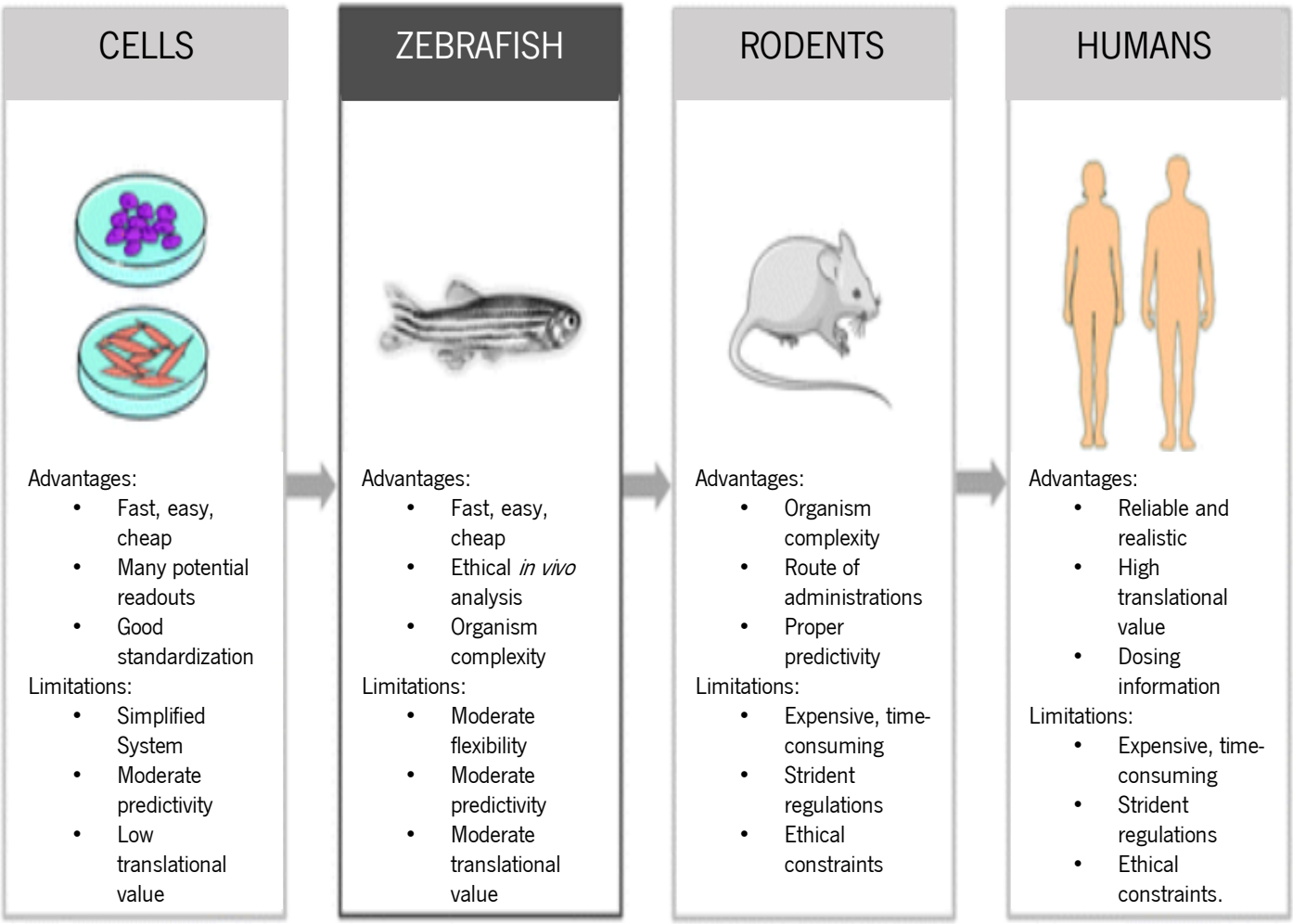

Figure 7. Experimental models passive of being used in scientific research [68].

Given the complexity of neurological disorders, such as AD, and the limited knowledge that one has about them, it I essential to conduct appropriate research in the laboratory, using animal models that are suitable as models for these diseases in order to facilitate the analysis of the mechanisms involved in such disorders [3], [76]. In the last two decades, several animal models have been used to study AD, with the aim of understanding the pathology, dynamics and molecular mechanisms involved in the disease. Rodents have already been used extensively in order to provide information in the context of pharmaceutical treatments for AD, however, it has recently been concluded that although rodents exhibit behaviors and anatomy similar to the human model of AD, they exhibit different transcriptional profiles, lacking consistency as a model. Therefore, new

animal models have emerged which can be used to study the neurobiology of this disease and possible treatments. Zebrafish is one of the most promising animal models for the study of a wide variety of disorders related to the nervous system, including in scientific work involving neurodegenerative diseases, such as AD, enabling the modeling of symptoms and their severity [3], [6]. This work was based on studies in cellular models.

1.4.1. Cell viability assays

The rate of proliferation and viability of cells are representative indicators of cell health. In order to keep these variables, as well as the cell death rate, under control, toxicity and cell viability assays can be performed. There are four main groups among which we can classify these tests, based on the basic principles of each method: Dye exclusion assays, Colorimetric assays, Fluorometric assays and Luminometric assays (Table 3).

Table 3. Description of several methods for determination of cell viability.

Assays		Description	Ref.
Dye Exclusion	Trypan Blue; Congo Red; Eosin.	It determines the number of viable cells on the basis that membranes of the viable cells are intact and therefore exclude dyes, unlike what happens in dead cells that internalize it. Thus, the evaluation of viability is made by observing the cells and by the ratio between the number of cells with a clear cytoplasm (living cells) and with the stained cytoplasm (dead cells).	[86]–[88]
Colorimetric	MTT assay; MTS assay; XTT assay.	This method is based on the reduction of a tetrazolium salt to a colored formazon product. This reaction occurs only in metabolically active cells. Through absorbance measurement, it is possible to establish a relationship between the amount of formazon product and the number of living cells, since they are directly proportional.	[83], [86], [89], [90]

Fluorometric	AO/PI; Resazurin	Fluorometric assays achieve a much higher sensitivity than the other methods. The fluorescent signal of the fluorescent dyes is measured in order to determine the ratio of viable and non-viable cells.	[86], [91]
Luminometric	ATP assay; Real time viability assay.	This method is based on the relation that exists between the luminescent reaction and the effect of the added compound. The addition of the reagent produces a light signal, generated by the chemical or biological reaction that happens, and this signal has the advantage of being a persistent and stable signal.	[92], [93]

1.5. OBJECTIVE

The discovery of the effects of both curcumin and siRNA in AD was the opening of a new world of possibilities. The studied beneficial effects of the curcumin and siRNA in the brain, more specifically in AD treatment, alongside the capability of the liposomes to carry these molecules through all the obstacles may represent a major breakthrough for this pathology research if effective delivery is successfully achieved.

The objectives were to formulate liposomes capable of encapsulating curcumin and siRNA, to evaluate the cytotoxicity of the liposomes in cell lines and to evaluate the neuroprotector effects of these nanoparticles also in cell lines.

To try and get a deeper knowledge of the real-time impact of these molecules and of these carriers, relevant cell models were used in this work.

2. Materials and Methods

2.1. MATERIALS

In Table 4 are described the materials that were necessary for the realization of this work.

Table 4. Products and respective suppliers.

Products	Supplier
Cholesterol;1,2-dioleoyl-3-dimethylammonium-propane (DODAP); Dipalmitoylphosphatidylcholine (DPPC); N-palmitoyl-sphingosine-1-{succinyl[methoxy(polyethylene glycol)2000]} (PEG ceramide);Sphingomyelin	Avanti Polar Lipids (Alabaster, AL)
Fetal Bovine Serum (FBS); Penicillin/Streptomycin	Biochrom GmbH (Berlin, Germany)
siRNA targeting TAU (5' rCrArUrCrCrArUrCrArUrArArArCrCrArGrGrATT'	Integrated DNA Technologies (Leuven, Belgium)
The RiboGreen® kit	Invitrogen (Eugene, OR)
Absolute Ethanol	Merck (Darmstadt, Germany)
Citric Acid; N-(2-Hydroxyethyl)piperazine-N'-(2-ethanesulfonic acid) (HEPES buffer);Sodium Citrate; Dulbecco's Modified Eagle's Medium (DMEM); *Curcuma longa*	Sigma-Aldrich (St Louis, MI)
Infinity Cholesterol®	Thermo Fischer Scientific (Waltham, MA)

2.2. BUFFERS

2.2.1. HEPES buffer preparation

For HEPES 20 mM + NaCl 150 mM, 4.766g of HEPES and 8.766g of NaCl were weighed. Subsequently, 800 mL of ultrapure water was added to the salts and the solution was vigorously mixed. After that, the solution's pH was measured and set to 7.4, with NaCl 1M or HCl 1M, depending on the initial pH value. An adequate volume of ultrapure water was added in order to reach the final volume of 1 L.

2.2.2. Citrate buffer preparation

For the citrate buffer, 0.2941g of sodium citrate dihydrate and 0.210g of citric acid monohydrate were weighed. After that, the salts were dissolved in 80 mL of ultrapure water. Afterwards, the solution's pH was measured and set to 3.0. In order to achieve a final volume of 100 mL, an adequate volume of ultrapure water was added to the solution.

2.3. LIPOSOME PREPARATION

The liposomes used were formulated using the following lipids: Cholesterol, Dipalmitoylphosphatidylcholine (DPPC), Sphingomyelin and PEG-ceramide. Also, for the formulations with 1,2-dioleoyl-3-dimethylammonium-propane (DODAP), it was also used DODAP.

2.3.1 Lipid solutions

For the preparation of the lipid solution, Cholesterol, Dipalmitoylphosphatidylcholine (DPPC), Sphingomyelin and PEG-ceramide, were weighed according to Table 5 and subsequently dissolved in 1 mL of absolute ethanol. The solutions were then heated and mixed in the vortex and stored at -20°C until further use.

Table 5. Lipids included in the liposomal formulation and respective concentration and mass to be diluted.

Lipid	Concentration (mM)	Mass (g) to be dissolved in 1mL solvent
Cholesterol	40 mM	0.015
DPPC	30 mM	0.022
Sphingomyelin	30 mM	0.019
PEG-Ceramide	20 mM	0.052

For the formulation of liposomes with DODAP, a solution of DPPC 30 mM in chloroform was prepared by weighting the previously mentioned weight, dissolving this mass in 1 mL chloroform.

2.3.2. Curcumin solution

For the preparation of the curcumin solution to be encapsulated in the liposomes, 3.68mg of curcumin 10mM were weighed. Afterward, this mass was dissolved in 1 mL of absolute ethanol followed by heating. The solution was then mixed in the vortex and stored at -20°C.

2.3.3. Liposomes without DODAP

All liposome solutions were prepared by ethanolic injection: 400 μL of the lipid's solution, consisting of a mix of 162.5 μL of cholesterol, 130 μL of DPPC, 65 μL of sphingomyelin and 32.5 μL of PEG-ceramide, were added dropwise under continuous mixing in the vortex, in aliquots of 60 μL to a 600 μL hepes buffer solution. In the intervals between aliquots the solutions were kept in a water bath set at 60°C, which is above the phase transition temperature of lipids.

2.3.4. Liposomes with DODAP

For liposomes containing DODAP, a film with 82.5 μL of DODAP and 84 μL of DPPC (both previously dissolved in chloroform) was made in the rotary evaporator. The remaining lipids were later added to the film. Subsequently, the lipid solution was added dropwise and under continuous mixing in the vortex, in aliquots of 40 μL to a 400 μL citrate buffer solution. Between aliquots the solutions were kept in a water bath set at 60°C. Since DODAP has a positive charge at acid pH but a neutral charge at a pH of 7.4, liposomes with DODAP are prepared in citrate buffer at pH 3.

2.3.5. Curcumin-encapsulated liposomes

The encapsulation of drugs into the liposomes has been studied for various decade and it has been proven to show some positive results such as minimizing the toxic effects of the free drug alone, the extension of the therapeutic effect of the drug and also it helps the therapeutic effect to last longer [77]. Curcumin was chosen due to its already studied benefits related to AD's disease [62].

In order to prepare curcumin-encapsulating liposomes, 65 μL of curcumin were added to the lipids mix in the previously described formulations, due to its hydrophobic nature.

2.3.6. siRNA-encapsulated liposomes

The siRNA-encapsulated liposomes were not formulated without DODAP.

For the preparation of siRNA-encapsulating liposomes, 10.25 μL of siRNA sense and 10.25 μL of siRNA antisense were added to the buffer solution, in the hepes buffer for the formulation without DODAP, and in the citrate buffer for the formulation with DODAP.

2.3.7. Mixture of curcumin-encapsulated liposomes and siRNA-encapsulated liposomes

Previous work performed within our research group regarding co-encapsulation of curcumin and siRNA showed that the encapsulation efficiency of the co-encapsulation is much lower than the separated-encapsulation, this mixture of liposomes was prepared by mixing curcumin-encapsulated liposomes with siRNA-encapsulated liposomes, previously formulated.

In this work, when used a mixture of curcumin-encapsulated liposomes and siRNA-encapsulated liposomes, it is always in a ratio of 1:1.

2.4. LIPOSOME PURIFICATION

The separation of the encapsulated fraction from the free fractions is a crucial step, to prevent the free fractions to interfere with the later quantification of the encapsulated and also to make sure that the size of our sample is as homogenous as possible. The danger in the purification process is the possible loss of small amounts of liposomes, so it has to be a careful process) [56], [57].

2.4.1. Molecular Exclusion Column

For the preparation of the molecular exclusion column, for liposomes purification, ultrapure water was used to wash the column for the first two times. This procedure was performed by adding the water carefully in circular movements. Subsequently, 3 mL of Sepharose gel, previously deaerated, was added. When it settled, the same amount of HEPES buffer was slowly dropped.

These steps were then repeated until the column was filled with the sepharose gel. As sepharose gel was added, the top of the column was being lifted with a spatula to prevent the formation of layers.

2.4.1.1. Size Separation Chromatography

The method used for the purification of liposomes was the size separation chromatography. Due to the size of the liposomes prepared, the gel used for the molecular exclusion column was the Sepharose gel.

For the procedure, first of all, the column was washed by filling it completely with HEPES, previously filtered with a 0.22 μm filter, two to three times. Subsequently, after all the HEPES went down the column, 300 μL of the liposomal solution were added in the column and the remaining space was filled with filtered HEPES buffer. As the drops began to appear dull, they were collected to an eppendorf. The transparent drops were discarded.

2.5. LIPOSOMES QUANTIFICATION

During the purification through the molecular exclusion column there was an alteration of the lipid concentration due to the dilution. To assess the amount of curcumin and siRNA that was encapsulated in the liposomes and therefore to know the efficiency of the encapsulation it was necessary to perform lipid quantification, to accurately calculate the lipid concentration in the liposomes. This calculation consists in the determination of the concentration of the cholesterol.

For total lipid content quantification in the liposomes, the cholesterol concentration in the liposomes was measured by InfinityTM® cholesterol method. Since this lipid accounts for 50% of total lipid content, a simple conversion was then made. For this, two reaction mixes were prepared: one for the standards and one for the samples, according to the protocol. The calculations for standard preparation were made. In each well of the plate the adequate volume of a 0.25 mg/mL cholesterol standard starting solution was mixed with cholesterol buffer in order to reach the final concentrations of 1, 2.5, 5, 10 and 20 μg per well. 50 μL of the reaction mix was then added to each well.

For the sample wells, 50 μL of the sample were added, followed by the addition of the corresponding reaction mix, reaching the final volume of 100 μL.

The absorbance at 570 nm was measured in a microplate reader (SPECTRAmax PLUS® by Molecular Devices).

2.5.1. Curcumin quantification

In the first place, both liposomes with and without DODAP were passed through the molecular exclusion column to separate the free curcumin from the encapsulated curcumin.

Secondly, for curcumin quantification in the liposomes, the cholesterol concentration in the liposomes was measured. Since this lipid accounts for 50% of total lipid content and the curcumin accounts for 10% of total lipid content, a simple conversion was made.

Twelve black eppendorfs were prepared: six to add empty liposomes with DODAP and six to add empty liposomes without DODAP, all labelled according to the percentage of curcumin expected (0%, 25%, 50%, 75%, 100%, 200%). Apart from the lipids, curcumin solution and HEPES were also added to each eppendorf, according to the calculations previously made, and the mixes were incubated in the Thermoblock, for 1h at 60°C. Immediately after, a short spin in the vortex was performed and 100 μL from each of the eppendorfs were transferred to a fluorescence plate, in duplicate, for measurement in a fluorimeter, at λexc=420 nm and λem=520 nm.

2.5.2. siRNA quantification

The chosen method for the siRNA quantification in this work was through the measurement of fluorescence, using a probe that labels siRNA. To achieve this, it was necessary to disrupt the liposomes for the siRNA to be released.

2.5.2.1. Lysis of the liposomes for siRNA quantification

For siRNA quantification in the liposomes, the first step was the lysis of the liposomes. For that, we prepared two eppendorfs, one for the control and one for the liposomes. In the eppendorf for the control was added 135 μL of RNase free water and 15 μL of Triton 10x and in the one for the liposomes was added 133.5 μL of RNase free water, 15 μL of Triton 10x and 1.5 μL of purified liposomes with encapsulated siRNA. After this, the eppendorfs were kept in a water bath, at 60°C, for 20 s, then were transferred to a vortex, for a 10 s spin and lastly were kept in ice, for 20 s. This sequence was performed three times.

2.5.2.2. Encapsulated siRNA quantification

After the lysis of the liposomes, a RiboGreen® assay was performed in order to determine the encapsulation efficiency. The calculations for the standard preparation were made, according to the percentage of siRNA expected to be encapsulated (0%, 25%, 50%, 75%, 100%, 200%). In

each well of the fluorescence plate were added the appropriate volumes of siRNA and RNase free water, in order to complete 100 μL. After that, in each well were also added 100 μL of RiboGreen®.

The fluorescence was then measured at λexc=420 nm and λem=520 nm, in a fluorimeter.

2.6. LIPOSOME SIZE, PDI AND SURFACE CHARGE MEASUREMENT

For addressing liposomal size and polydispersity (PDI), 10 μL of the liposomal solutions, one at a time, were diluted in 990 μL of hepes buffer and the solution was placed in a polystyrene cuvette. The size and PDI were measured with and an attenuator between 6 and 9 and the particles count rate always superior to 150 kcps.

From the previous solution, 800 μL were transferred to a zeta cuvette to measure the superficial charge.

The size, PDI and superficial charge measurements were also performed with a dilution of 10 μL of liposomes in 990 μL of distilled water.

2.6.1. Size and PDI determination by Dynamic Light Scattering (DLS)

All the previous size and PDI measurements were determined by Dynamic Light Scattering (DLS) on Malvern Zetasizer®. Dynamic Light Scattering is usually applied in the measurement of the size of the particles by measuring the Brownian motion of particles in a dispersion and with this information it determines their hydrodynamic size [78]. The Brownian motion of the suspended particles causes the laser light to be scattered with different intensities. The analysis of these intensity fluctuations results in the speed of Brownian motion and by using the Stokes-Einstein equation we obtain the particle size [78].

2.6.2. Surface Charge determination by Electrophoretic Light Scattering

All the surface charge measurements were determined by Electrophoretic Light Scattering (ELS) on Malvern Zetasizer®. Electrophoretic Light Scattering (ELS) measures the electrophoretic mobility of dispersed particles and this mobility is converted into zeta potential. The fundamental physical principle in these measurements is that of electrophoresis. The dispersion is injected into a cell that contains two electrodes and to which an electric field is applied. The particles that have a net charge migrate towards the opposite charge electrode with a velocity, known as mobility, that is related to their zeta potential [78].

2.6.3. Stability of liposomes

The stability of liposomes was measured on two different ways: the storage stability of the liposomes at 4°C and the stability of liposomes under 37°C.

2.6.3.1. Storage stability of liposomes at 4°C

Over time, liposomes tend to fuse with each other and form aggregates, assuming a state that is thermodynamically their most stable state. However, a change at this level causes changes in the properties of liposomes, which results in a different final product with different characteristics from those previously outlined [58]. The formation of aggregates results in particles bigger than what they are supposed to be, making the liposomes ineffective. In addition, as the work was carried out with liposomes with encapsulated drugs, a fusion of the liposomes could result in leakage of the encapsulated.

With this, the storage stability was measured one time a week during the first month and then monthly. The empty, curcumin-loaded and siRNA-loaded liposomes were kept at 4°C during this time.

For these measurements, 10 μL of liposomes were diluted in 990 μL of HEPES buffer in a plastic cuvette and the size and PDI were measured.

2.6.3.2. Stability at 37°C

Since the finality is to study the impact of liposomes in AD, and to try and mimic the conditions of the human body, the stability of the liposomes was measured at 37°C which is the human body temperature. Following this, to measure the stability at 37°C were also added other variables, related with alterations in the pH. According to the literature, one of the causes related to the accumulation of the TAU and the amyloid-β is a malfunction at the level of the endosomes, which are responsible for the transport of these proteins [79]. The pH of the endosomes is located at around 5, so the stability of the liposomes was measured at pH 5, at a pH of 7.4, which is around the value of the blood pH, and also at pH 7.4 in a solution of 10% Fetal Bovine Serum (FBS). There are studies that report the relation between the amyloid-β and the presence of FBS, in which the accumulation of Aβ decreases in the presence of this serum [80].

So, for this procedure, the stability at 37°C of curcumin-loaded liposomes with and without DODAP was measured with the liposomes in a solution of HEPES pH 7.4, in a solution of HEPES

pH 5 and in a solution of 10% FBS. The stability of the liposomes under different environments was measured by controlling their size, PDI and surface charge at certain predefined timepoints. These measurements were performed at 0h, 3h, 6h, 8h, 10h, 24h, 28h and 32h. The timepoints were defined based on the literature, which states the short half-life of liposomes. Studies show that liposomes can have a half-life of up to 24h in rats and up to 45h in humans. These times may change depending on the formulation of the liposomes [52], [81], [82].

For the measurements, 100 μL of liposomes were diluted in 9900 μL of HEPES 7.4 and were placed in a water bath at 37°C. In each timepoint (0h; 3h; 6h; 8h; 10h; 24h; 28h; 32h) an aliquot of 1 mL was taken from the solution and placed in a plastic cuvette and the size and PDI of the sample was read in the Zetasizer. Subsequently, 800 μL were transferred to a zeta cuvette to measure the superficial charge. This procedure was then repeated with the HEPES pH 5 and with 10% FBS.

2.7. CELL CULTURE

2.7.1. L929 cell line

The mouse embryonic cell line (L929) (NCTC clone 929 [L cell, L929, derivative of Strain L] (ATCC® CCL1™)) was chosen due to their great use for the evaluation of nanoparticles and its cytotoxicity. In addition, it is reported in various studies, that L929 is one of the most widely used cell lines in toxicity studies due to its high growth rates and biological responses [83].

The mouse embryonic cell line (L929) was cultivated in Dulbecco's Modified Eagle Medium (DMEM), supplemented with 10% (v/v) of inactivated fetal bovine serum (FBS) and 1% (v/v) of antibiotic/antimycotic. The cells were maintained in 25 cm^2 cell culture flasks, in an incubator with 5% CO_2, set to 37°C. In order to maintain its properties, the cells were subcultured in 25 cm^2 cell culture flasks using 0.05% trypsin, before reaching confluence.

To avoid microbial and cross-contaminations, all the assays were performed under sterile conditions in a laminar flux chamber and with sterile equipment.

2.7.1. SH-SY5Y cell line

SH-SY5Y cell line (ATCC® CRL-2266™) is a neuroblastoma cell line and is used as a reliable model for assays to test the neurotoxicity or neuroprotection of drugs. The advantages associated with the use of this cell line are associated with its ability to differentiate into a neuron-

like phenotype and some of the benefits of this cell line capacities are the possibility of a large-scale expansion being low cost to culture when in comparison with primary neurons, these cells are considered a cell line therefore there are no ethical concerns associated to its culture and since they are human-derived they are able to express some specific human-proteins that would not be present in other primary cultures [84], [85].

The SH-SY5Y neuroblastoma cell line was cultivated in a mixture (1:1) of Dulbecco's Modified Eagle Medium (DMEM) and Ham's F12 nutrient, supplemented with 10% (v/v) of inactivated fetal bovine serum (FBS) and 1% (v/v) of antibiotic/antimycotic. These cells were maintained in 25 cm^2 cell culture flasks, in an incubator with 5% CO_2, set to 37°C. In order to maintain its properties, the cells were subcultured in 25 cm^2 cell culture flasks using 0.25% trypsin, before reaching confluence.

2.7.2. Cell viability assays

For this work, the chosen methods were the Methyl Tetrazolium (MTT) cytotoxicity assay, for the evaluation of the metabolic activity, and the Acridine Orange (AO) and Propidium Iodide (PI) assay, for the evaluation of the membrane's integrity and to distinguish between apoptotic and viable cells.

2.7.2.1. MTT cytotoxicity assay

MTT assays were performed to assess cell viability by measuring the proliferation of L929 after the incubation with different liposomal formulations at different concentrations. This was possible since the mitochondrial enzymes digest the tetrazolium salt to a colored formazan product, a reaction that happens only in metabolic active cells. Despite the downside of the formazan being insoluble in water and therefore requiring DMSO or isopropanol to solubilize the crystals, which ends up increasing the error between wells, MTT has the advantage of being highly reproductive and also being safe and easy to perform [83]. It can be used to determine cytotoxicity as well as cell viability, through the evaluation of the metabolic activity, which makes it a good assay even in the face of other assays [94].

L929 cell line was plated at the density of $4.72x10^3$ cells/well in a 96 well plate and were left to adhere for 24h in an incubator, at 37°C, with 5% CO_2. After 24h of incubation, the medium was removed and the various liposomes, at different concentrations, in duplicates, dissolved in medium were added. A negative control, containing only medium, and a positive control, containing

30% (v/v) of Dimethyl Sulfoxide (DMSO) in medium, were also tested, both in duplicate. As soon as the desired time of incubation was over (24h; 48h), the liposomes were removed and a solution of MTT and medium (1:5) was added to the cells. After 2h of incubation, at 37°C, the solution was removed and a mixture of ethanol/DMSO 1:1 was added to dissolve the formazan crystals. A little mixing was performed and subsequently 100 μL of each well were transferred, in triplicate, to a 96 well absorbance plate and the absorbance was measured at λ_{Ex}=570 nm and at 630 nm as a background control.

2.7.2.2. AO and PI assay

In addition to the MTT assay to determine cell viability the AO and PI assays were also carried out together, for the determination of cell viability and cell non-viability, respectively. These methods are needed because despite the target of the mitochondria for the metabolic activity assessment, there is also the need to target nucleic acids, to assess the membrane integrity as well as to obtain the ratio between apoptotic and viable cells [91].

AO is a membrane-permeable dye that accumulates in acidic organelle structures, such as the lysosomes. Upon excitation with a blue light, it emits a green fluorescence. To complement this fluorescent dye, PI was also used, which is membrane-impermeable nucleic acid marker, which means that it only stains if the membrane is compromised [91].

L929 cell line was plated at the density of $2.73x10^4$ cells/well in a 24 well plate and were left to adhere for 24h in an incubator, at 37°C, with 5% CO_2. After 24h of incubation, the medium was removed and the various liposomes, at different concentrations, dissolved in medium, were added. A negative control, containing only medium, and a positive control, containing 30% (v/v) of Dimethyl Sulfoxide (DMSO) in medium, were also tested. As soon as the desired time of incubation was over (24h), the liposomes were removed and a solution of PI 50 μg/mL was added and incubated in the dark, at 37°C, for 15 minutes. After that time, a solution of AO 50 μg/mL was added to the plate and incubated for another 15 minutes, in the dark, at 37°C. At the end of that time, the fluorescence was visualized in a fluorescence microscope, using FITC and TRITC filters. To quantify the living cells, the ones stained green, and the dying cells, the one stained red, was used as a tool the software Image J.

2.8. ACETYLCHOLINESTERASE (AChE) ACTIVITY

For this assay, SH-SY5Y cell line was plated at the density of $6.8x10^4$ cells/well in a 48 well plate and were left to adhere for 24h in an incubator, at 37°C, with 5% CO_2. After 24h of incubation, the medium was removed, discarding the floating cells, and the various liposomes, at different concentrations, in duplicates, dissolved in medium were added. The controls tested in these assays were only medium, EtOH 100mM, EtOH 500mM, t-BHP 1mM and H2O2 1mM. As soon as the desired time of incubation was over (24h), each well was washed with PBS and the cells were de-adhered with trypsin 0.25%. Subsequently, the cell suspension was washed with a solution of cold PBS, 5% FBS to inactivate the trypsin. The content of each well was transferred for a 96 well absorbance plate, in triplicate, and in each of these wells was added 100 μL of 0.5 mM DTNB (Ellman's Reagent) and ATCh (Acetylthiocholine) and the absorbance was measured every ten minutes for one hour at λ_{Ex}=410 nm.

2.9. STATISTICAL ANALYSIS

One-way ANOVA model with Dunnet's multiple comparisons was used to analyze size and superficial charge of the formulations of liposomes with or without DODAP, as well as to analyze the cytotoxic effects of the liposomes on L929 cell line with MTT and PI/AO assays.

A *P* value of 0.05 was used for significance testing. Statistical analysis was generated in GraphPad Prism 8.

3. Results

3.1. SIZE, PDI AND SURFACE CHARGE

Liposomes were characterized based on their size, PDI and surface charge, by DLS. These measurements were performed on empty liposomes, on curcumin-loaded liposomes and on siRNA-loaded liposomes.

For optimal systemic application of the liposomes, their ideal size is below 200 nm and the PDI should be between 0 and 0.2 to guarantee a homogenous population [35], [40].

3.1.1. Empty liposomes

The samples of the liposomes were analyzed before and after the purification using the molecular exclusion column (Figure 8 and Table 6).

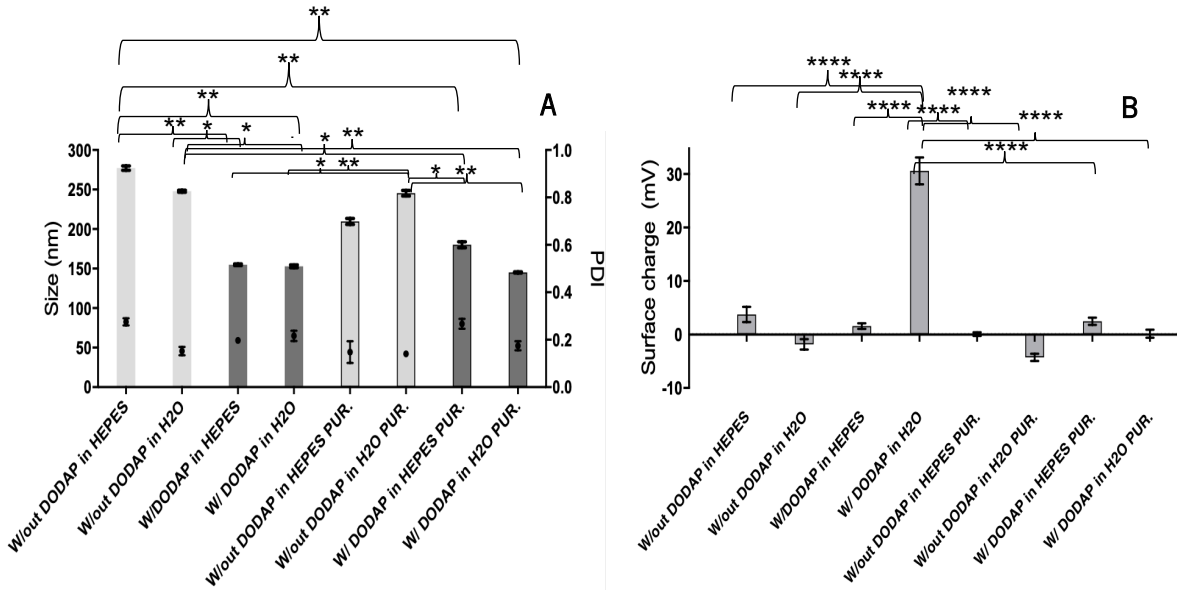

Figure 8. Size (bars), PDI (dots) (A) and surface charge (B) of the empty liposomes, before and after purification.
* Statistically significant according to One-Way ANOVA with Dunnet's multiple comparison test ($P < 0.05$).

Table 6. Mean and Standard Deviation of size and surface charge of empty liposomes. W/out, without; w/, with; PUR, purified.

	SIZE		CHARGE	
	Mean	SD	Mean	SD
W/OUT DODAP IN HEPES	277.0	2.843	3.730	1.430
W/OUT DODAP IN H2O	247.8	1.356	-1.850	0.970
W/DODAP IN HEPES	154.9	1.084	1.550	0.534
W/DODAP IN H2O	152.9	1.881	30.60	2.510
W/OUT DODAP IN HEPES PUR	209.5	3.821	0.0539	0.346
W/OUT DODAP IN H2O PUR	245.3	3.641	-4.270	0.674
W/DODAP IN HEPES PUR	180.2	3.821	2.470	0.670
W/DODAP IN H2O PUR	145.0	0.9813	0.140	0.772

As we can see in Figure 8A, there are only a few variations in the values of size, PDI and surface charge between liposomes with and without DODAP. In a figure 8B, there is a major alteration in the liposomes with DODAP in water, that may be due to some interaction of the water with the systems.

3.1.2. Curcumin-loaded liposomes

The same procedure was applied to measure the size, PDI and surface charge of the curcumin-loaded liposomes (Figure 9 and Table 7).

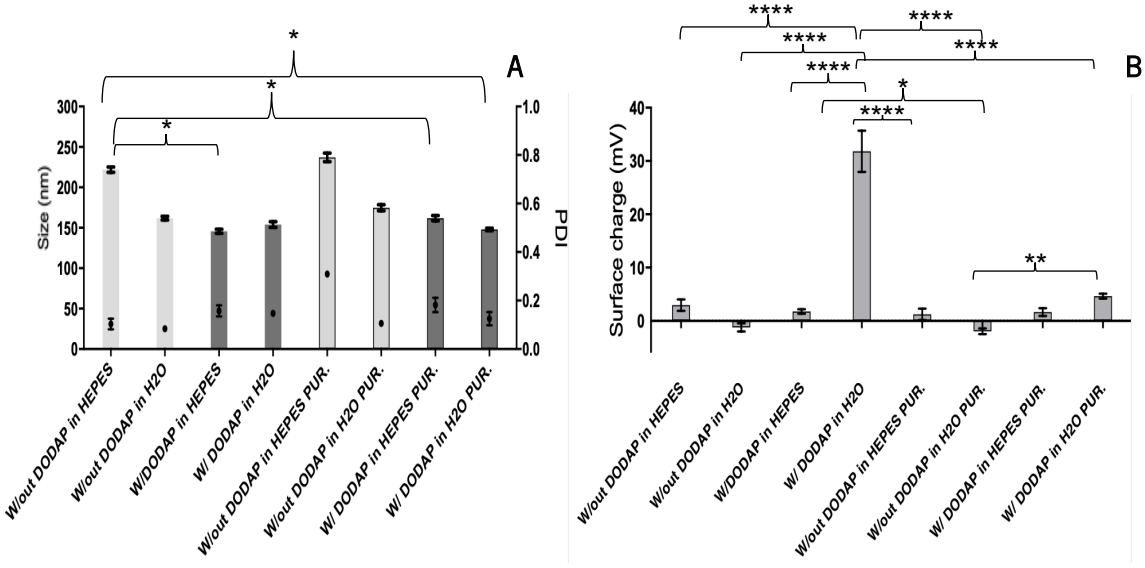

Figure 9. Size (bars), PDI (dots) (A) and surface charge (B) of the curcumin-loaded liposomes, before and after purification. * Statistically significant according to One-Way ANOVA with Dunnet's multiple comparison test ($P < 0.05$).

Table 7. Mean and Standard Deviation of size and surface charge of curcumin-loaded liposomes. W/out, without; w/, with; PUR, purified.

	SIZE		CHARGE	
	Mean	SD	Mean	SD
W/OUT DODAP IN HEPES	221.9	3.232	2.960	1.090
W/OUT DODAP IN H2O	162.0	2.400	-1.230	0.779
W/DODAP IN HEPES	145.8	2.555	1.750	0.448
W/DODAP IN H2O	154.1	3.639	31.80	3.870
W/OUT DODAP IN HEPES PUR	237.1	5.297	1.230	1.090
W/OUT DODAP IN H2O PUR	174.8	3.798	-1.960	0.540
W/DODAP IN HEPES PUR	161.9	3.298	1.660	0.756
W/DODAP IN H2O PUR	147.9	1.590	4.620	0.495

By comparing the results depicted in Figure 8 and Figure 9, it is possible to notice some differences in size and PDI, ranging from 150 nm to 250 nm and from 0.1 to 0.3, respectively. The liposomes need to rearrange in order to being able to encapsulate the curcumin, which is highly hydrophobic, and due to that, it is predictable that curcumin-encapsulated liposomes may display bigger size and higher PDI values. Similar to what happens in figure 8B, in figure 9B there is a major alteration in the liposomes with DODAP in water, that may be due to some interaction of the water with the systems.

3.1.3. siRNA-loaded liposomes

The samples of the siRNA-encapsulated liposomes were also analyzed, measuring the size, PDI and surface charge, in the same way as with the empty and the curcumin-encapsulated liposomes (Figure 10 and Table 8).

The comparison between the figures 8, 9 and 10 shows that the siRNA-encapsulated liposomes are smaller than the empty and the curcumin-encapsulated liposomes.

For the siRNA-encapsulated liposomes, were only used the formulations of liposomes with DODAP. The positive charge of DODAP interact electrostatically with the negative charge of siRNA, which results in a complex with the genetic material entrapped. [70].

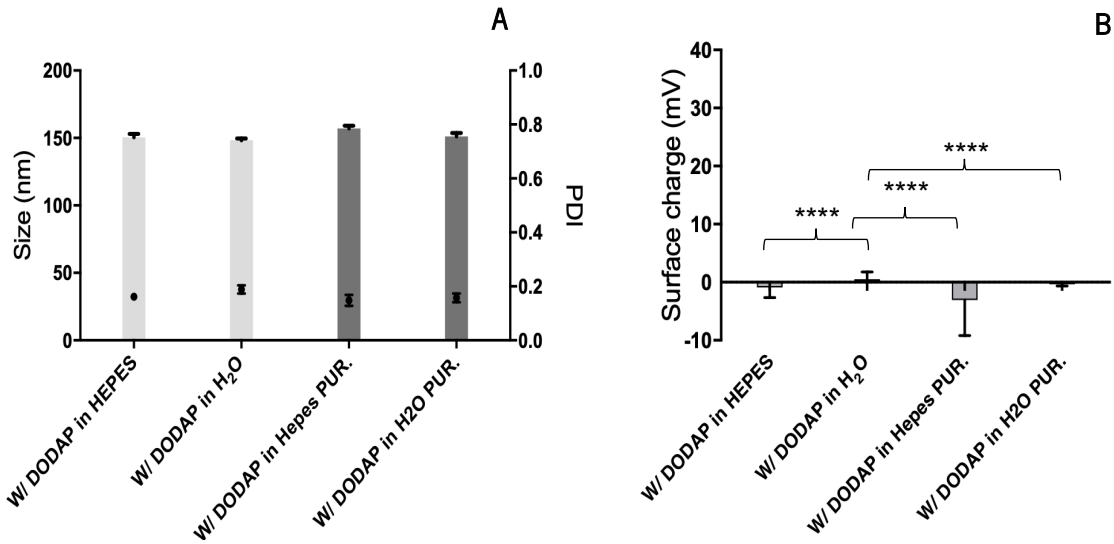

Figure 10. Mean size (bars), PDI (dots) (A) and surface charge (B) of the siRNA-loaded liposomes, before and after purification. **** Statistically significant according to One-Way ANOVA with Dunnet's multiple comparison test ($P < 0.05$).

Table 8. Mean and Standard Deviation of size and surface charge of siRNA-loaded liposomes. W/, with; PUR, purified.

	SIZE		CHARGE	
	Mean	SD	Mean	SD
W/DODAP IN HEPES	150.5	2.484	-0.901	1.760
W/DODAP IN H2O	148.2	1.491	0.502	1.270
W/DODAP IN HEPES PUR	157.0	2.018	-3.070	6.120
W/DODAP IN H2O PUR	151.2	2.423	-0.344	0.284

The siRNA-encapsulates liposomes are the smaller, when in comparison with the empty and the curcumin-loaded liposomes. This may be due to electrostatic interactions between siRNA and DODAP that lead to the formation of smaller liposomes.

3.1.4. Storage stability of liposomes

The empty, curcumin-loaded and siRNA loaded liposomes were stored at 4°C. Their stability was measured in the Zetasizer, once per week during the first month and then monthly. These measurements are important to assess the lifetime of nanoparticles, since if they are not stable during storage, they will not be stable under physiological conditions.

3.1.4.1. Empty liposomes stability

The storage stability of the empty liposomes was measured, as presented in Figures 11 and 12.

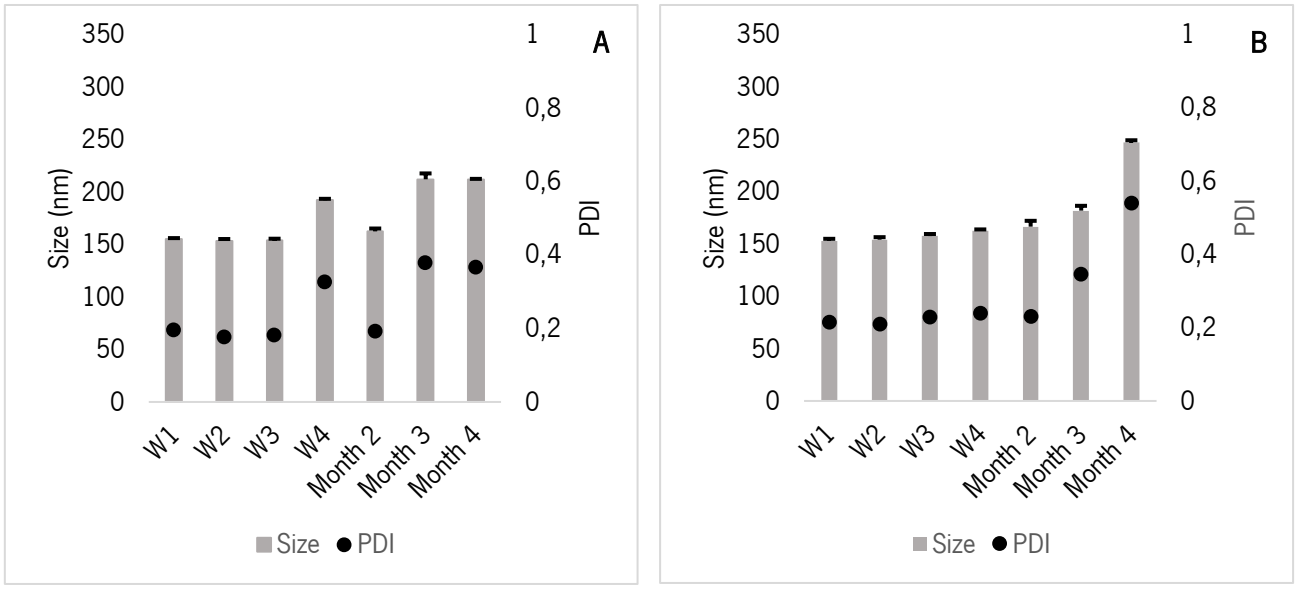

Figure 11. Size and PDI stability of empty liposomes with DODAP, measured in HEPES (A) and ultrapure water (B).

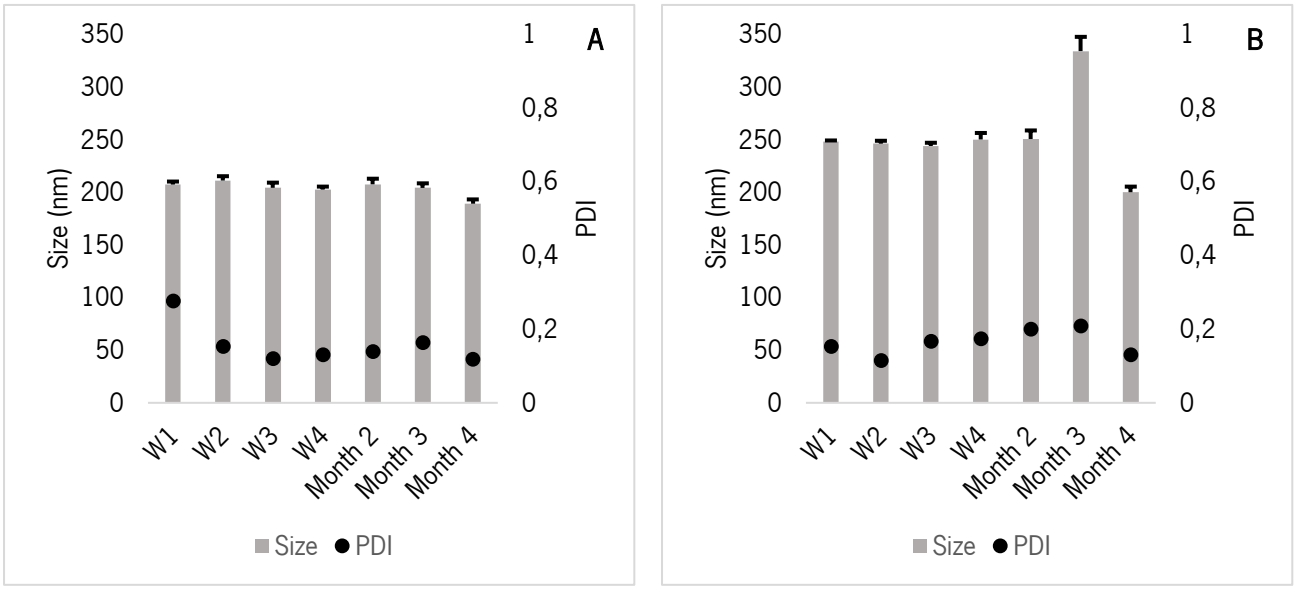

Figure 12. Size and PDI stability of empty liposomes without DODAP, measured in HEPES (A) and ultrapure water (B).

As we can see in Figures 11 and 12, the empty liposomes are quite stable up to three months. In the fourth month, some measurements show an increase of the size and PDI.

3.1.4.2. Curcumin-loaded liposomes stability

The storage stability of the curcumin-loaded liposomes was measured, as presented in Figures 13 and 14.

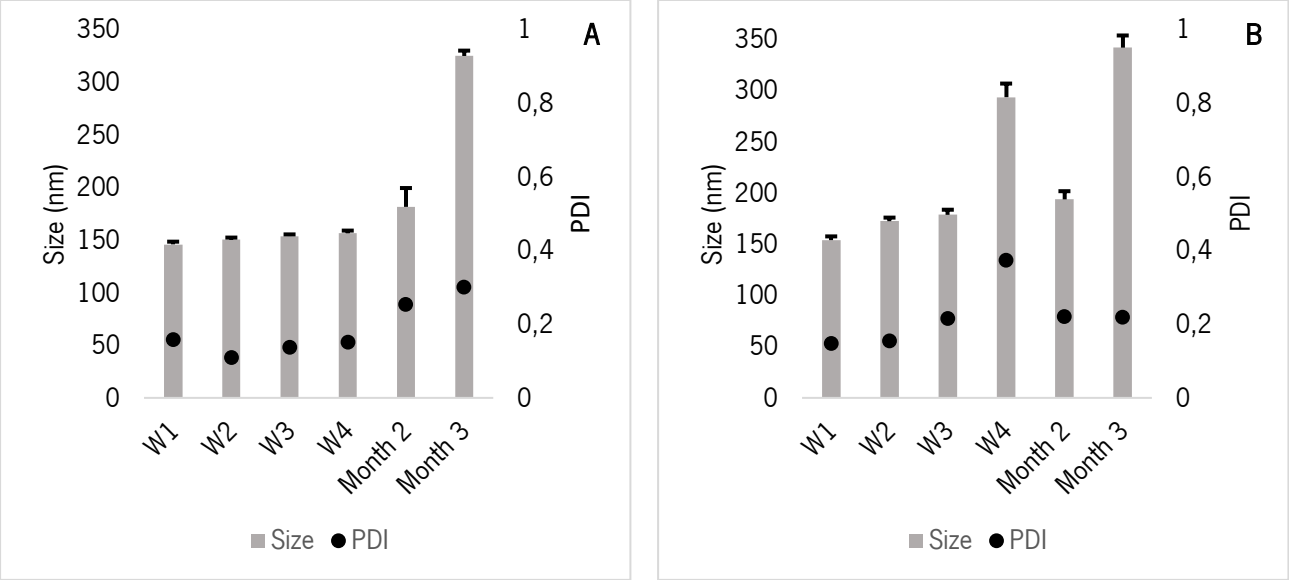

Figure 13. Size and PDI stability of curcumin-loaded liposomes with DODAP, measured in HEPES (A) and ultrapure water (B).

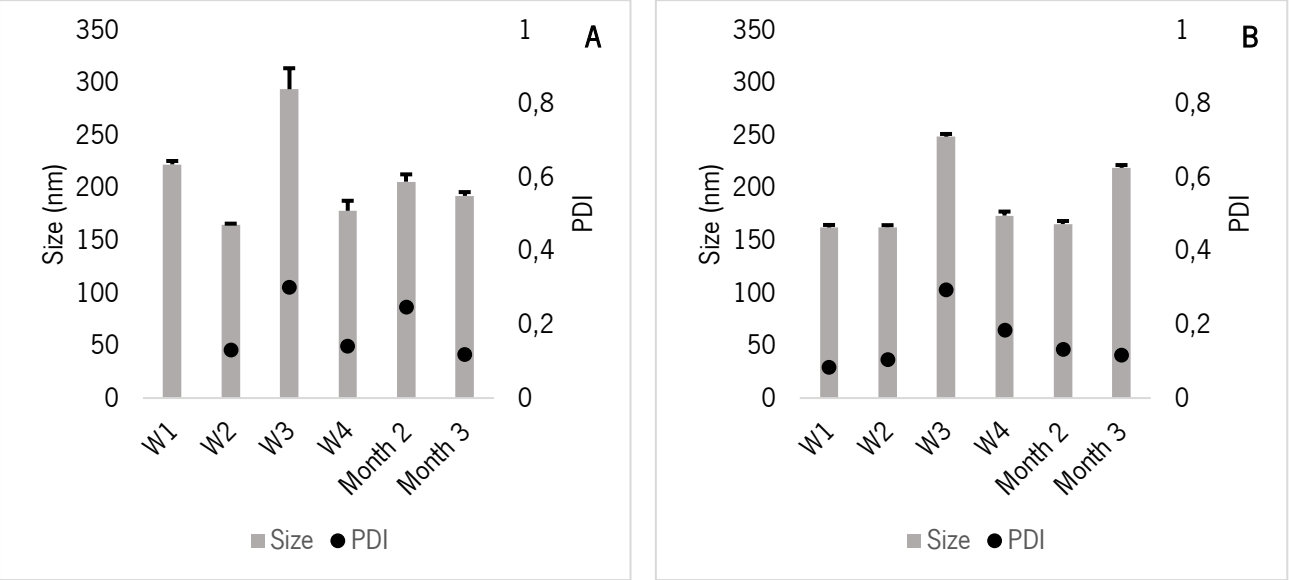

Figure 14. Size and PDI stability of curcumin-loaded liposomes without DODAP, measured in HEPES (A) and ultrapure water (B).

The measurements of the curcumin-loaded liposomes presented in Figures 13 and 14, shows that although curcumin liposomes are larger than the empty liposomes, they are quite stable up to three months. At the third month measurements the liposomes with DODAP appeared to start losing their stability.

3.1.4.3. siRNA-loaded liposomes stability

The storage stability of the siRNA-loaded liposomes was measured, as presented in Figure 15.

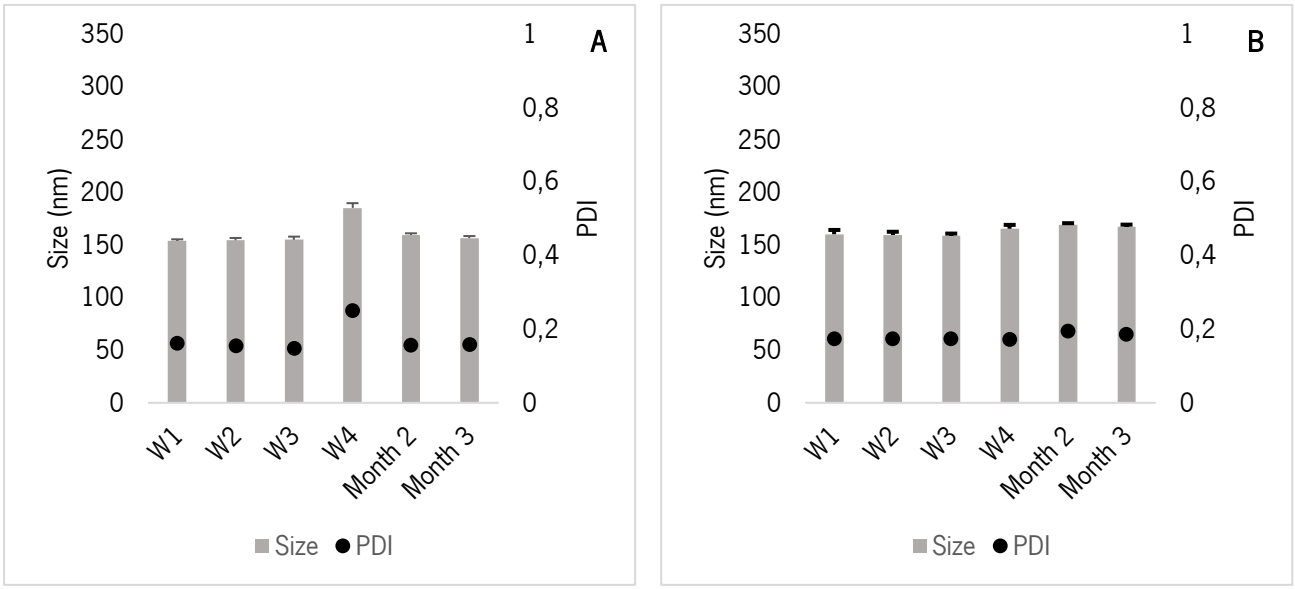

Figure 15. Size and PDI stability of siRNA-loaded liposomes with DODAP, measured in HEPES (A) and ultrapure water (B).

The formulation of siRNA loaded liposomes, as observed in Figure 15, remains stable, with almost no variations in size and PDI, up to three months. Possible due to the electrostatically interactions between DODAP and siRNA, these liposomes are more stable for a longer time.

3.1.5. Stability in physiological conditions

The stability of the curcumin-loaded liposomes, with and without DODAP, was measured over time, in different conditions: in HEPES pH 7.4, HEPES pH 5.0 and in 10%FBS, and at different timepoints (to assess short- and long-term stability).

3.1.5.1. At 37°C, in a solution of HEPES pH 7.4

In Figure 16, it is possible to see the evolution over time of the behavior of the curcumin-loaded liposomes, with and without DODAP, when diluted in a solution of HEPES buffer, at pH 7.4, at a temperature of 37°C, which mimics their circulation in the human body.

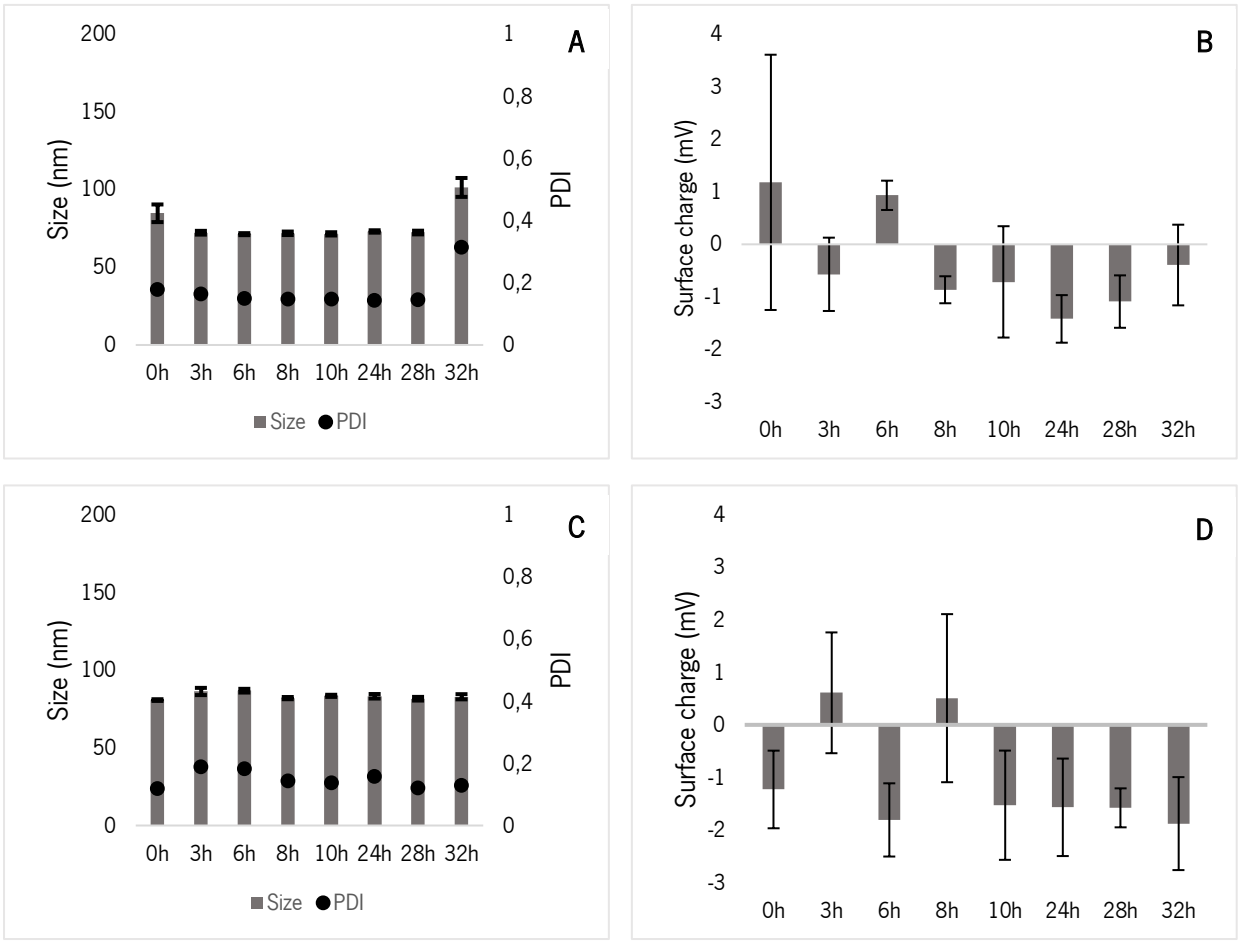

Figure 16. Size, PDI (A and C) and surface charge (B and D) of the curcumin-loaded liposomes with DODAP (above) and without DODAP (below), diluted in HEPES pH 7.4.

Through the analysis of the figure, it is possible to see that incubation at 37°C and pH 7.4 does not affect stability up to 28h. In the formulations with DODAP, in the last timepoint (32h) appears to occur a slight alteration which may mean that stability begins to be compromised. Overall, there are only a few minor changes in the values of the size, PDI and surface charge. Also, their size is around 100 nm, which is the ideal size not to clog blood capillaries during circulation.

3.1.5.2. At 37°C, in a solution of HEPES pH 5.0

The size, PDI and surface charge of the curcumin-loaded liposomes, with and without DODAP, when diluted in HEPES pH 5.0, was measured (Figure 17). Liposomes are internalized by endocytosis and end up in endosomes, whose pH is around 5.

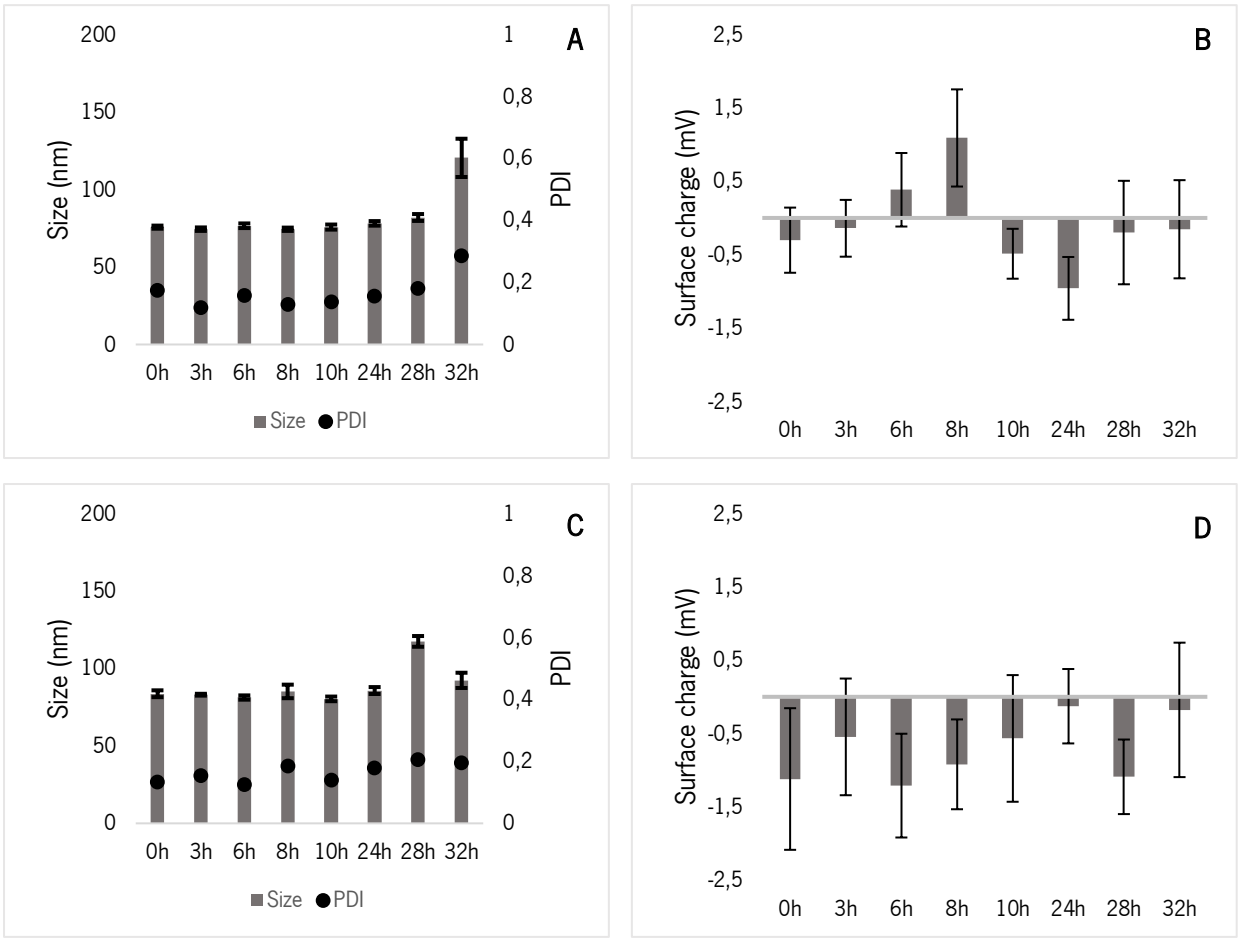

Figure 17. Size, PDI (A and C) and surface charge (B and D) of the curcumin-loaded liposomes with DODAP (A and B) and without DODAP (C and D), diluted in HEPES pH 5.

Looking at the Figure 17, it is possible to see that incubation at 37°C and pH 5 does not affect stability up to 24h. In graphic **A**, which refers to curcumin-loaded liposomes with DODAP, at 32h, there is a slight increase in size and PDI. By looking at graphic **C**, relative to the curcumin-loaded liposomes without DODAP, it shows an apparent variation in size, at 28h.

This differences between both graphics may be an indicator that the formulations with DODAP are stable for a longer period of a time, when comparing to the formulations without DODAP.

3.1.5.3. At 37°C and pH 7.4, in a solution of 10%FBS

The same procedure was repeated in 10%FBS (Figure 18). These liposomes have potential applications in the systemic circulation; therefore, it is important to predict how they will interact with proteins in the blood serum, hence the use of FBS.

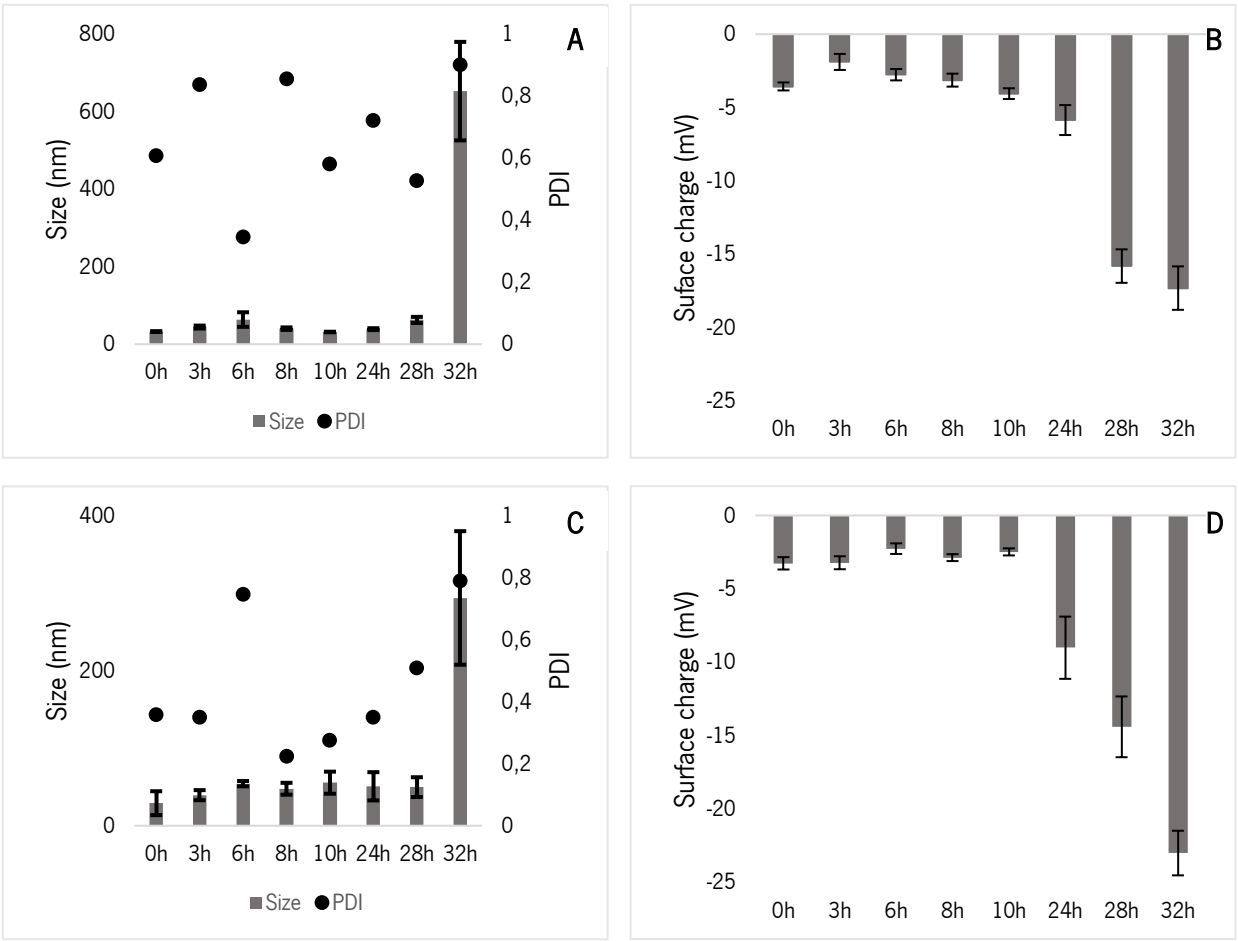

Figure 18. Size, PDI (A and C) and surface charge (B and D) of the curcumin-loaded liposomes with DODAP (A and B) and without DODAP (C and D), diluted in a solution of 10%FBS.

The results of the measurements of the size, PDI and surface charge of the liposomes in 10%FBS (Figure 18) show a clear loss of stability of the liposomes, especially after 28h.

In the superficial charge graphics, we observe significant changes. This may be due to interaction with proteins in the serum. The most abundant protein in FBS is albumin, a negatively charged protein. So, an interaction between this protein and the systems can result in a more negative charged environment.

3.2. ENCAPSULATION EFFICIENCY

The samples were analyzed before and after the purification in the molecular exclusion column. To assess the amount of curcumin and siRNA that were indeed encapsulated, the results between unpurified liposomes and purified liposomes were compared.

3.2.1. Curcumin

The results of the encapsulation efficiency of curcumin are shown in Table 9.

Table 9. Encapsulation efficiency of curcumin-loaded liposomes with and without DODAP (n=3).

LIPOSOMES	Encapsulation efficiency (%)
With DODAP	26.12
Without DODAP	45.96

3.2.2. siRNA

In Table 10 are shown the results of the encapsulation efficiency of siRNA. The siRNA is only encapsulated in liposomes with DODAP; therefore, the encapsulation efficiency of siRNA was only measured in liposomes with DODAP.

Table 10. Encapsulation efficiency of siRNA-loaded liposomes with DODAP (n=3).

LIPOSOMES	Encapsulation efficiency (%)
With DODAP	73.71

The results show an encapsulation efficiency of 73.71%, which is very satisfactory. This is in agreement with the results obtained when analyzing the zeta potential of liposomes with siRNA.

3.3. CELL VIABILITY

As we are developing systems with future biomedical applications it is important to evaluate the exposure of the cells to these systems. In order to assess the cell viability after the incubation of the liposomes in the L929 cell line were performed two assays: MTT assay and AO/PI assay.

3.3.1. MTT assay

In order to assess cell viability, on a metabolic perspective, a MTT assay was performed. As controls were used DMSO 30% as the death control and HEPES buffer, at the same percentage as the most concentrated liposome sample.

After the absorbance measurements, at 570 nm, the percentages of cell survival obtained were normalized to the negative control, the HEPES buffer (100% viability). The results were presented in percentage of survival for each time point (24h and 48h).

In this assay were analyzed different samples: empty liposomes, with and without DODAP, curcumin-loaded liposomes, with and without DODAP, siRNA-loaded liposomes, with DODAP, and also the mixture of curcumin-loaded liposomes, with and without DODAP, with the siRNA-loaded liposomes, and at different concentrations ($1x10^{-6}$M, $1x10^{-4}$M, $2x10^{-4}$M). The results are shown in Figure 19.

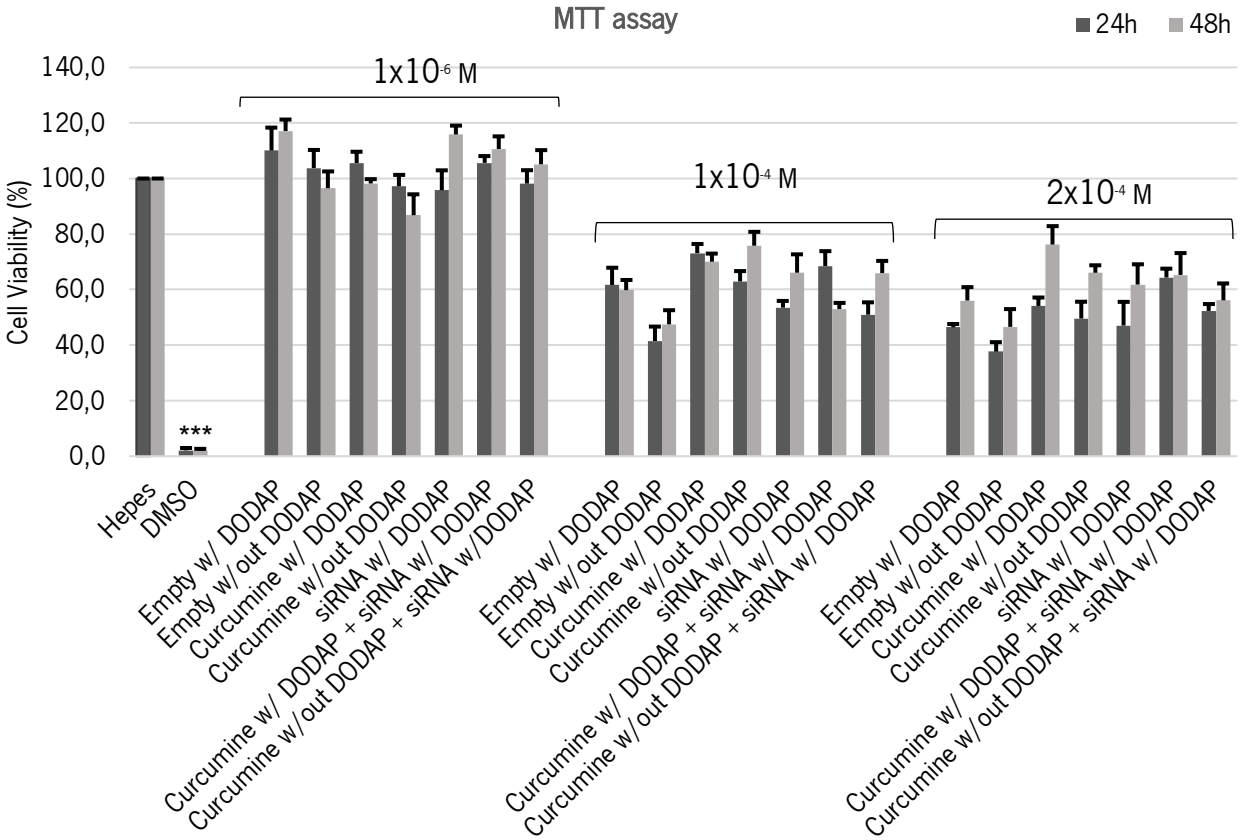

Figure 19. Cell viability of the different formulations of liposomes in L929 cell line, at different concentrations (1x10-6M, 1x10-4M, 2x10-4M), determined by MTT assay. *** Statistically significant with respect to the control group according to One-Way ANOVA with Dunnet's multiple comparison test ($P < 0.001$).

The results show that liposomes at the lower concentrations ($1x10^{-6}$M) are the least toxic to the cells, with a cell viability rate of around 100%. The two other concentrations show relatively similar values in terms of percentage of cell viability: at a concentration of $1x10^{-4}$M was obtained a percentage of cell viability of approximately 60%/70% and for the higher concentrations ($2x10^{-4}$M) it is around 50%.

It is also possible to see that although cell viability was measured at two different times, 24h and 48, the results are not so different from one another, which indicates that cytotoxic effect occurs immediately, without triggering any prolonged effect mechanisms, and that cells do not recover from the initial effect.

3.3.2. AO and PI assay

The AO and PI assay were performed in order to distinguish between apoptotic and non-apoptotic cells. As described previously, the AO emits a green fluorescence, indicating the living cells, and the PI emits a red fluorescence, which indicates the death cells (Figure 19).

The amount of cells survival was normalized to the negative control (100% viability) and expressed in percentage (Figure 19). In the lower concentration of liposomes ($1x10^{-6}$M), it is possible to observe that cell viability is above 80%, which is the reference value below which it can be considered a cytotoxic effect. In the two other concentrations, $1x10^{-4}$M and $2x10^{-4}$M, a decreasing tendency in cell viability can be observed, resulting in values around 50%. This decreasing tendency is noticeable in all formulations, regarding the encapsulated content.

3.3.2. AO and PI assay

The AO and PI assay were performed in order to distinguish between apoptotic and non-apoptotic cells. As described previously, the AO emits a green fluorescence, indicating the living cells, and the PI emits a red fluorescence, which indicates the death cells (Figure 21).

The amount of cells survival was normalized to the negative control (100% viability) and expressed in percentage (Figure 20).

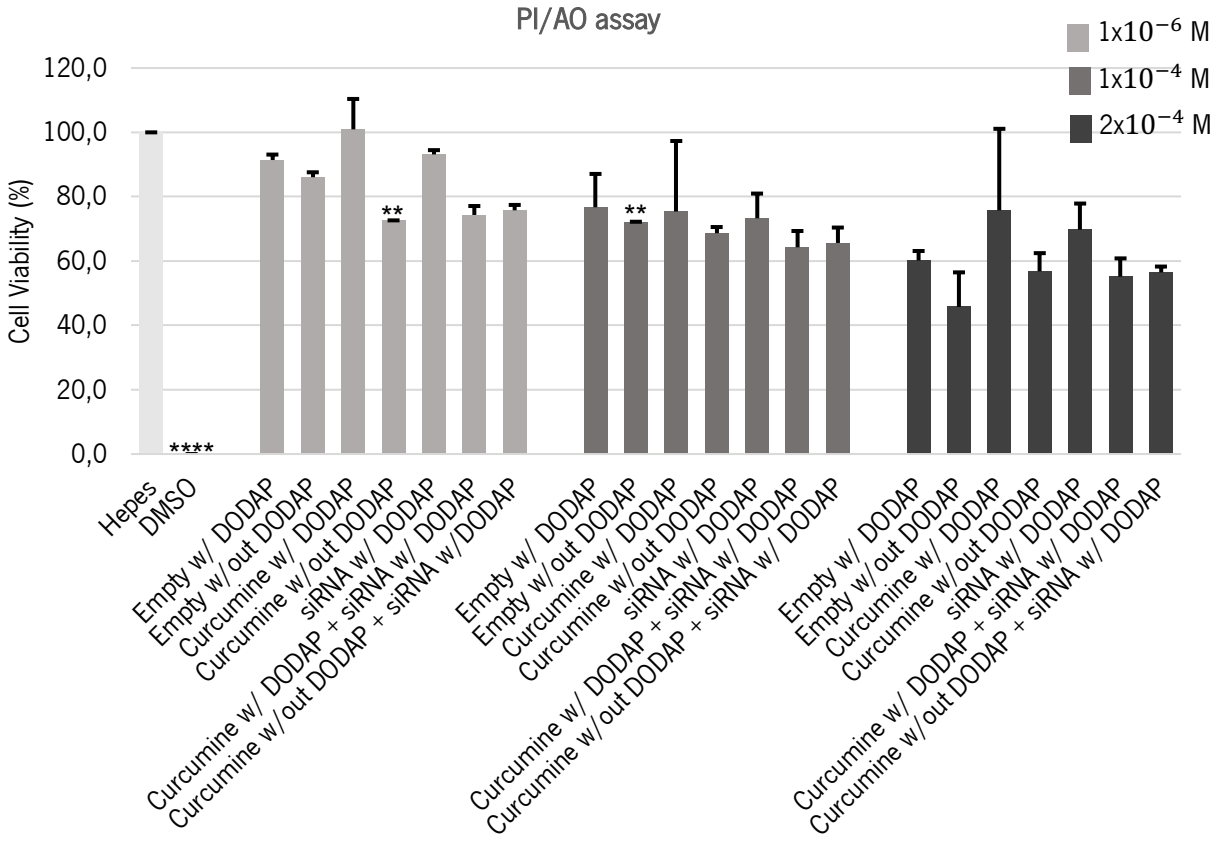

Figure 20. Cell viability of the different formulations of liposomes in L929 cell line, at different concentrations (1x10-6M, 1x10-4M, 2x10-4M), determined by PI/AO assay. **/**** Statistically significant with respect to the control group according to One-Way ANOVA with Dunnet's multiple comparison test ($P < 0.05$).

The results obtained in AO are in agreement with the results obtained in MTT. Looking at this figure, it is possible to observe that in general, in all liposome formulations, as the concentration of liposomes increases, the percentage of cell viability decreases. This indicates that the liposomes toxicity increases with increasing concentration.

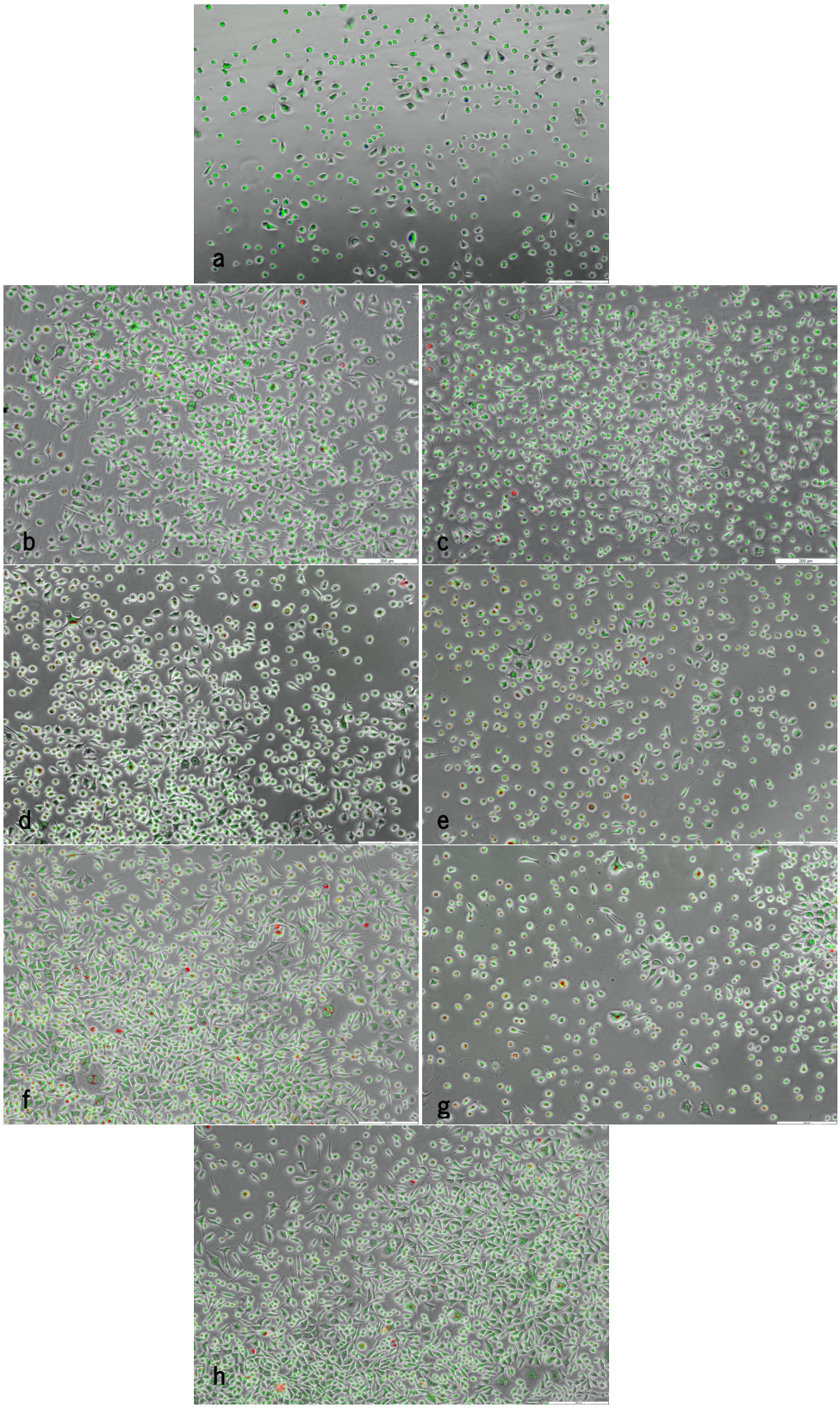

Figure 21. L929 cells, 24 hours after incubation with a) only HEPES; b) empty liposomes with DODAP; c) empty liposomes without DODAP; d) curcumin-loaded liposomes with DODAP; e) curcumin-loaded liposomes without DODAP; f) mixture of curcumin-loaded liposomes with DODAP and siRNA-loaded liposomes; g) mixture of curcumin-loaded liposomes without DODAP and siRNA-loaded liposomes; h) siRNA-loaded liposomes, all at the concentration of $1x10^{-6}$ M.

By the analysis of the Figure 20 and Figure 21 it is possible to observe that the toxicity of liposomes shows almost no change whether the liposome formulations are with DODAP or without DODAP. It is also clear that in Figure 21, as indicated by the graphic, the lower concentrations show almost no red dots, which means a cell viability close to 100%.

3.3.3. Comparison between MTT and PI/AO

The results of the MTT assay and the PI/AO assay were grouped to identify differences in cell viability between both assays (Figure 22), since MTT evaluates the metabolic cell viability and PI/AO discriminates between viable and apoptotic cells.

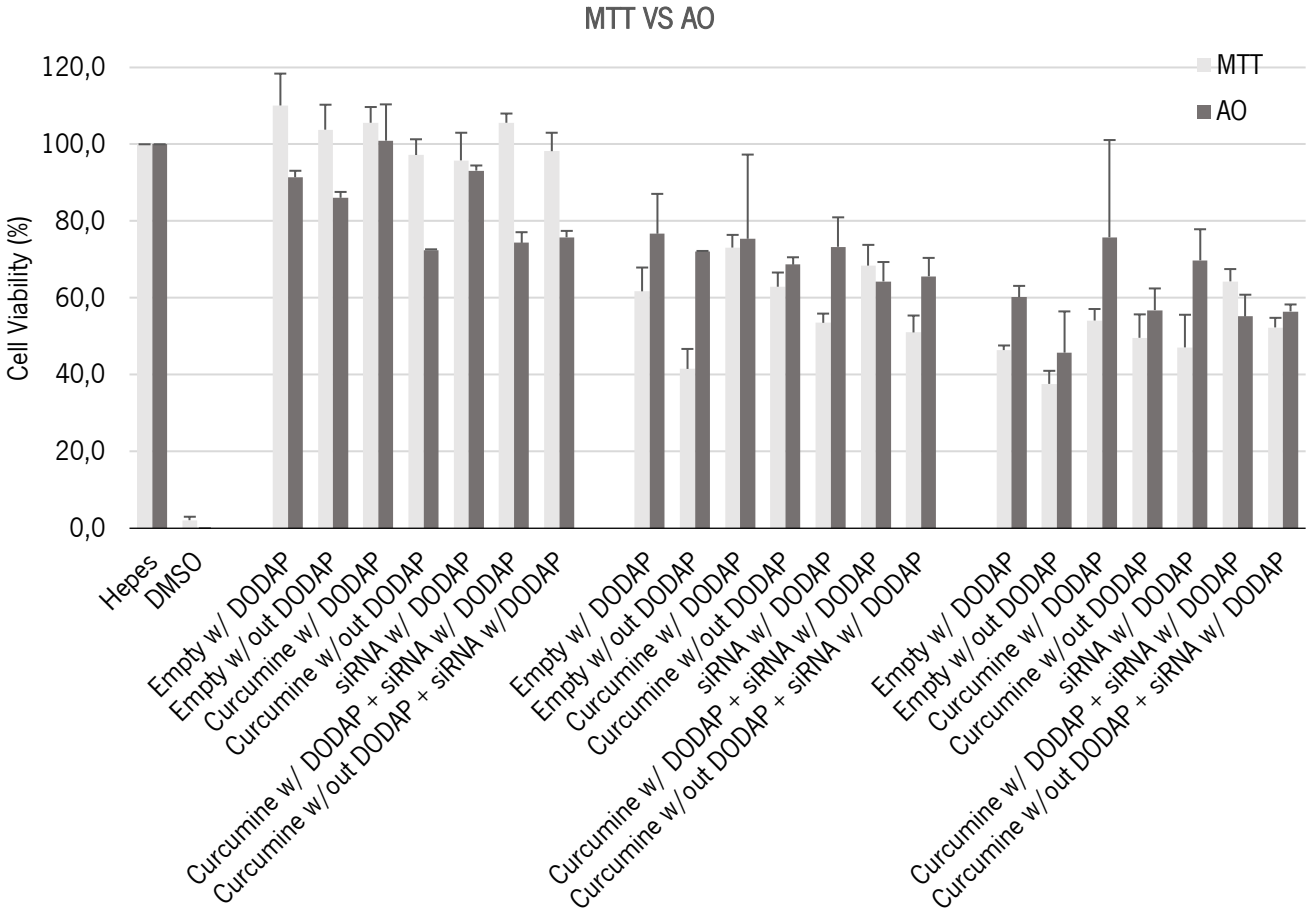

Figure 22. Comparison between MTT and PI/AO assays.

There is low disparity between assays, however it is perceptible some differences in the results from each one, especially in the lower concentrations, which leads to the conclusion that PI/AO assay is more sensible than MTT assay.

3.4. ACETYLCHOLINESTERASE ACTIVITY

In order to determine the acetylcholinesterase activity and if the compounds are able to inhibit it or not, the acetylcholinesterase activity assay was performed. In this assay were used four controls: the only medium, EtOH 100 mM, EtOH 500 mM, t-BHP 1mM and H_2O_2 1mM.

The acetylthiocholine used in the last step of the methods was used as a substrate because it is specific for AChE, otherwise we wouldn't know for sure if the results were showing AChE activity. In this assay were analyzed different samples: empty liposomes, with and without DODAP, curcumin-loaded liposomes, with and without DODAP, siRNA-loaded liposomes, with DODAP, and also the mixture of curcumin-loaded liposomes, with and without DODAP, with the siRNA-loaded liposomes, and at different concentrations ($1x10^{-6}$M, $1x10^{-4}$M, $2x10^{-4}$M). The absorbance was measured at 410 nm and the results are shown in Figure 23, 24, 25 and 26.

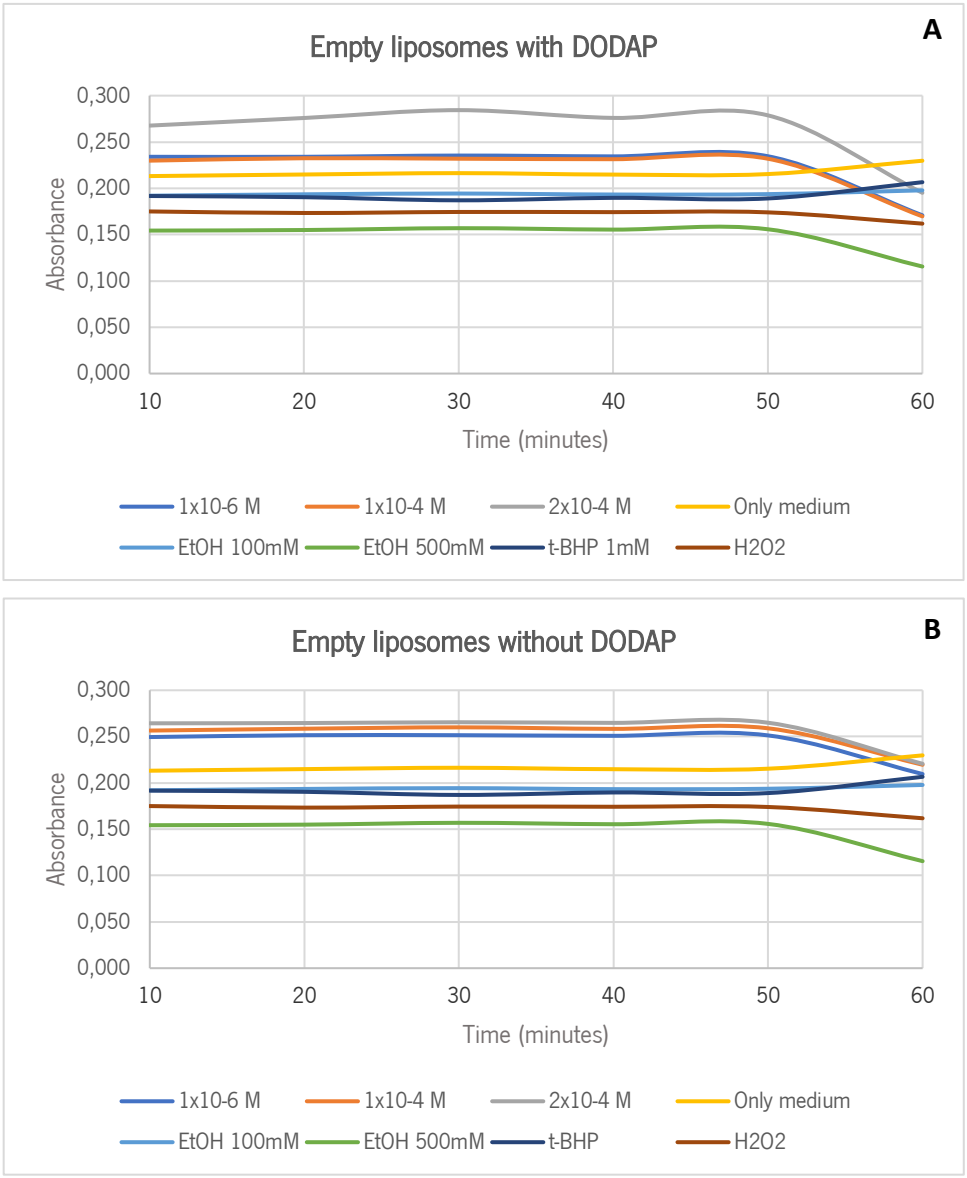

Figure 23. Acetylcholinesterase activity at different timepoints in empty liposomes with (**A**) and without (**B**) DODAP, at different concentrations (n=3).

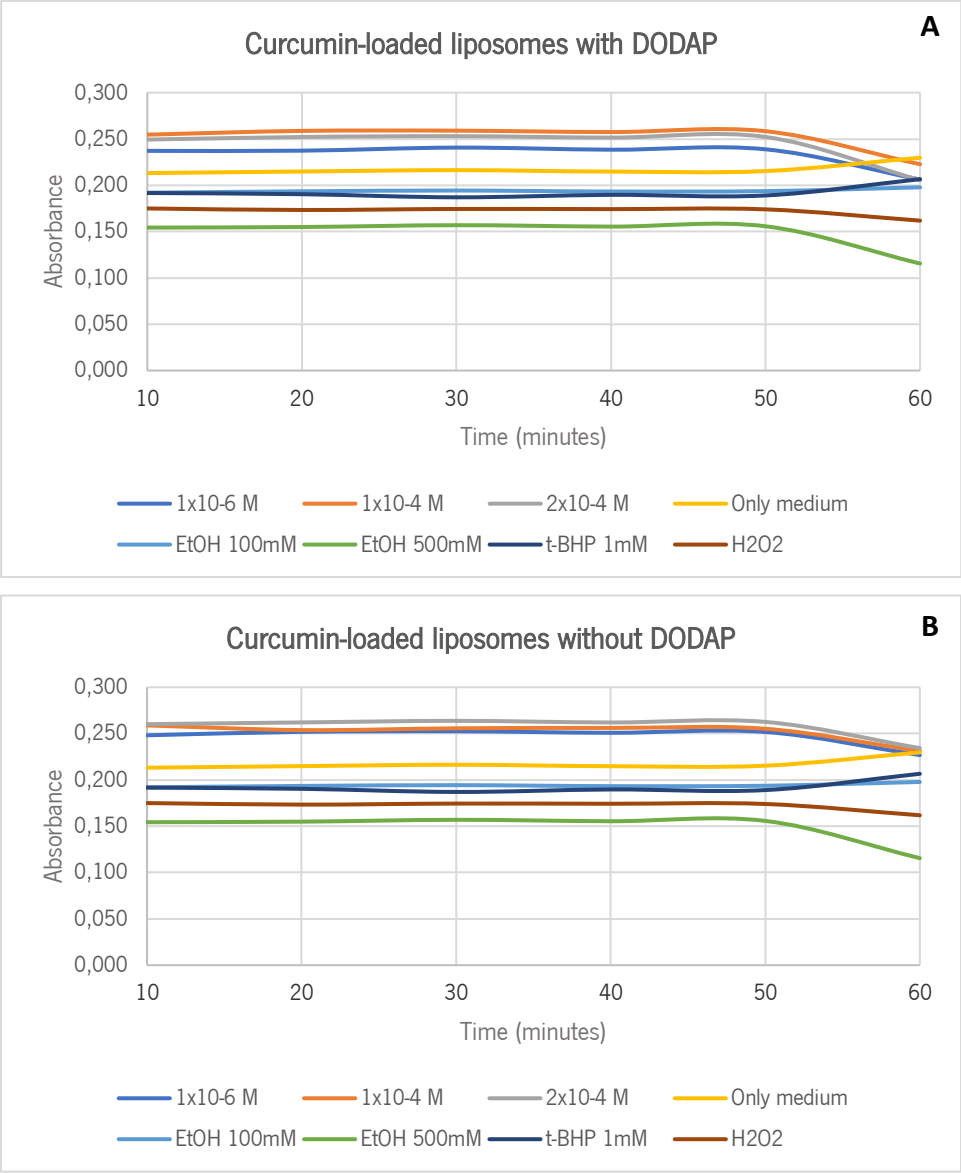

Figure 24. Acetylcholinesterase activity at different timepoints in curcumin-loaded liposomes with (**A**) and without (**B**) DODAP, at different concentrations (n=3).

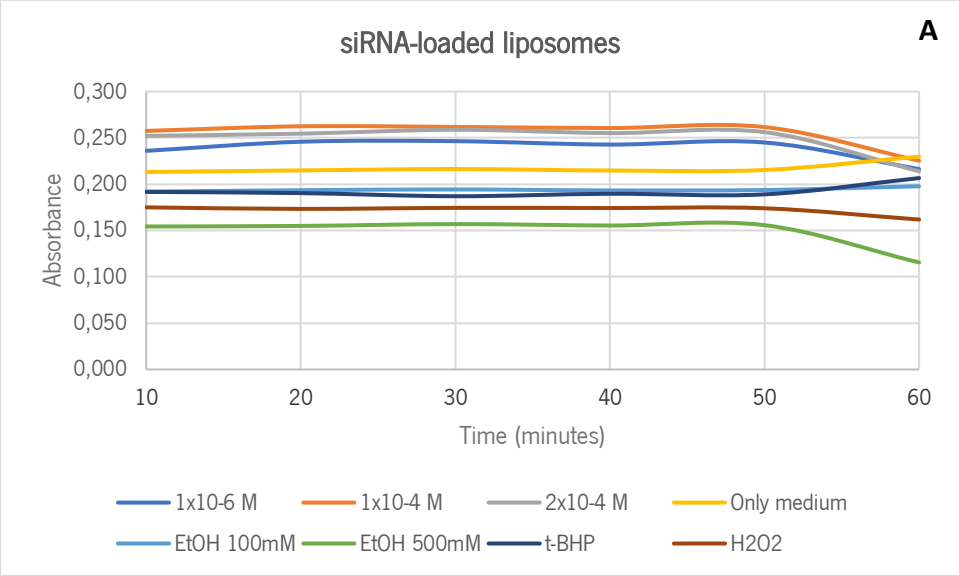

Figure 25. Acetylcholinesterase activity at different timepoints in siRNA-loaded liposomes with DODAP, at different concentrations (n=3).

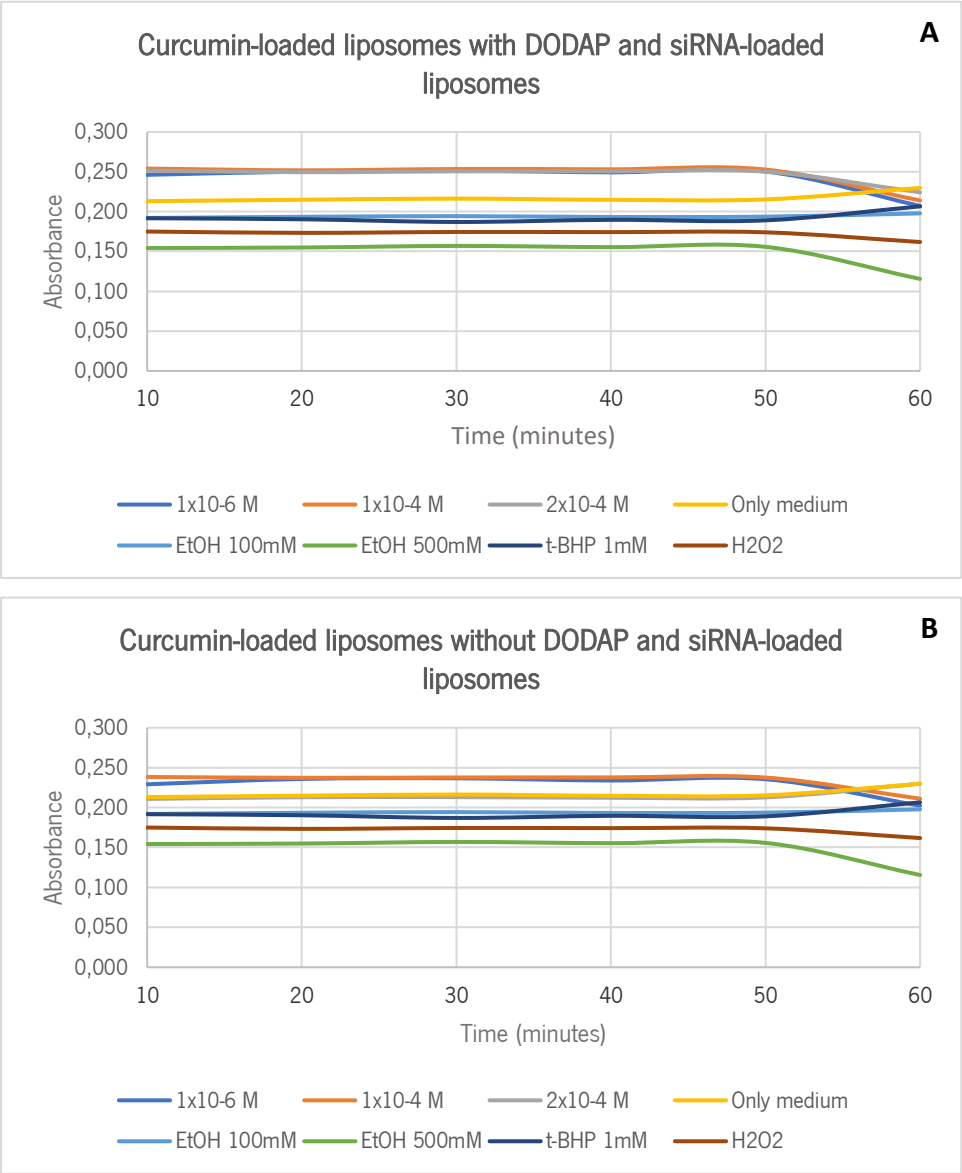

Figure 26. Acetylcholinesterase activity at different timepoints of the mixture of siRNA-loaded liposomes with curcumin-loaded liposomes with (A) and without (B) DODAP, at different concentrations (n=3).

In the previous figures (23 to 26) are represented the graphics corresponding to the results of the acetylcholinesterase activity. As controls were used t-BHP, H_2O_2, Ethanol 100 mM and 500 mM. According to the literature, H_2O_2 and t-BHP induce acetylcholinesterase activity, and it happens especially after 50 minutes of reaction. Ethanol 500 mM should display a higher activity, however as it is very toxic to the cells, we deduced that it caused high mortality therefore there are fewer cells producing a signal.

As for the liposomes, it is possible to observe that in the first 50 minutes they show a higher acetylcholinesterase activity, when in comparison with the controls, however its tendency

line starts to decrease at 50 minutes of reaction, which can be an indicator of some inhibition of the acetylcholinesterase activity.

Also, by the results expressed in Figure 26, and comparing with the results obtained in Figures 24 and 25, it is possible to observe that the mixture of curcumin-loaded liposomes with siRNA loaded liposomes does not have any different impact in the inhibition of acetylcholinesterase activity – its behavior is almost the same as the curcumin-loaded liposomes and the siRNA-loaded liposomes individually.

4. Discussion

The results obtained by Cheng *et al* [95], that formulated curcumin-loaded liposomes with cholesterol and phospholipids in the formulation, through ethanol injection method, were similar to the results obtained in this study as the size of the liposomes obtained was also under 200 nm and the PDI was around 0.2. The encapsulation efficiency was also similar, around 46%, that was the value we obtained in the curcumin-loaded liposomes without DODAP. Moreover, Mokhtarieh *et al* [96] prepared siRNA-loaded liposomes with similar composition, although through a different method, and the values of size, PDI and encapsulation efficiency obtained by them were 120 nm, 0.174 and 86.5%, respectively, similar to the ones obtained in this study.

Liposomes, with or without DODAP, when encapsulating curcumin and siRNA display some alterations in the values of size, PDI and surface charge in comparison with the empty liposomes. Notwithstanding, the size of the liposomes remained under 200 nm, the ideal size not to provoke any clog in blood capillaries, and the PDI was under 0.2, so the samples weren't very polydisperse [35]. The liposomes appeared to be stable up to at least three months, similar to what was obtained by Haghiralsadat *et al* [97] that prepared siRNA-loaded liposomes with an identical formulation.

Regarding the cytotoxic assays performed in the L929 cell line, analysis of the cell viability percentage on the MTT assay suggests that the cell metabolism was not affected neither by the liposomes nor by curcumin and siRNA. Also, the difference of the cell viability of the curcumin-loaded and the siRNA-loaded liposomes when compared to the empty liposomes is almost none, which led to the conclusion that the loaded liposomes are not more toxic than the empty ones. However, some of the formulations present some degree of toxicity, that is, a cell viability percentage below 80%. The results shown in Figure 17 suggest a dose dependent effect, being the highest cell viability percentage achieved at the concentration of $1x10^{-6}$M. This happens in both liposomal formulations, with and without DODAP.

According to Cui *et al* [98], cationic liposomal formulations show an increased cellular toxicity due to their capacity of activating some pro-apoptotic and pro-inflammatory cascades. However, from the results in Figure 17 we see that the formulations with DODAP, a cationic lipid, show a lower cytotoxicity than the ones without DODAP in their formulations and it happens not only in the empty liposomes but also in the curcumin- and siRNA-loaded liposomes. This possibly occurs because we use low concentrations of DODAP and also because DODAP is a cationic lipid known to be of low cytotoxic. Also, according to several studies, and as Cui *et al* [98] corroborated,

liposomes with DODAP in their formulations are known to be less toxic than liposomes with other cationic lipids in their formulations. This molecule is also known to have a positive charge only when in an acidic environment (pH of 3.0 or lower) and although the liposomes with DODAP are formulated in citrate buffer, at pH 3.0, they are later purified in the molecular exclusion column with filtrated HEPES buffer, at pH 7.4, which could neutralize the charge of the molecule, lowering its cytotoxic effects in the cells.

The positive charge of DODAP is of high importance to the encapsulation of siRNA. Without DODAP in the liposomal formulations it is not possible to encapsulate siRNA because what entraps the siRNA are the electrostatic interactions that happen with the cationic lipid [70]. So, for siRNA to be trapped inside of liposomes, the process has to be performed in an acidic environment. For this to be possible it is used the citrate buffer (pH 3.0) so that DODAP can keep its positive charge. Another positive side of the DODAP molecule being positive only at an acidic pH and neutral at a physiological pH is that it avoids nonspecific an undesirable interactions when in contact with human serum [73].

The data above is corroborated by the results in Figure 18, of the PI/AO assay. As Byvaltsev *et al* [91] reviewed, AO stains the living cells because it diffuses through the cytoplasmic membrane and binds to DNA producing a green fluoresce. PI is a dye that can be used to complement the results obtained from the AO, since PI is a fluorescent compound that accumulates in dying cells where the membranes are already compromised [93] and produces a red fluorescence. So, in Figure 20 we can see the results from the MTT and PI/AO compiled and it shows only slightly differences between them. The differences observed can derive from a wide number of variables, but as Jaszczyszyn and Gąsiorowski [99] discussed it can occur because of MTT assay. MTT relies on a mitochondrial enzyme to convert the tetrazole to formazan crystals so the generated signal is dependent on the level of cell metabolism and there are many variables that can affect the metabolism, for example, culture conditions, if cells are confluent it can reduce its growth therefore reducing the metabolism levels, or there can be other molecules that are able to interact with MTT and form the formazan product producing an higher absorbance [100]. It is for all these reasons mentioned that when the MTT is carried out, the PI/AO is also carried out, so that the data can complement and lead to the most reliable results possible.

From the results of cytotoxicity acquired and shown in Figures 17, 18 and 20 we move on to cytotoxicity in Zebrafish. Fernandes *et al* [101] study published recently crosses the bridge between *in vitro* and *in vivo* studies, applying similar liposome formulations to zebrafish embryos.

Similar to our results, in Fernandes *et al* study HEPES buffer showed no significant toxicity to the zebrafish at no stage of development. Also, in their study the cumulative survival percentage was between around 75% and 95% which is relatively similar to the results shown in Figure 20, although in the cells the cell viability ranges from smaller values (around 45%) to higher values (100%). Other similarity with the study of the liposomes in the cells and Fernandes *et al* study is that in general the liposomes with the lower concentrations appear to be less toxic than the ones with higher concentrations. And the toxicity increases with the passage of time, just as we can see in Figure 17, by the results of MTT at 24h and 48h.

A study reviewed by García-Ayllón *et al* [102] revealed that there is a connection between acetylcholinesterase, amyloid-β plaques and NFTs. It was found that in these regions, AChE is increased across all stages of the disease, including the early stages. Also, acetylcholinesterase is mainly located in cholinergic neurons,

The controls EtOH 100 mM, EtOH 500 mM, H_2O_2 and t-BHP used in this work are associated with a promoting effect on the AChE activity. In fact, Sun *et al* [103] performed an experiment using SH-SY5Y cell line incubated with EtOH from 50 mM to 500 mM and with H_2O_2, to study the alterations on the AChE activity, following an identical protocol to the one used in this work. The authors found out that the higher the ethanol concentrations, the higher the values of AChE activity. Furthermore, H_2O_2 was associated with even higher values of AChE activity.

Nonetheless, the results obtained in this work showed a lower AChE activity for the EtOH 500 mM and H_2O_2 over the EtOH 100 mM values, which can be explained by the increased pro-apoptotic effects of both EtOH 500 mM and H_2O_2 that consequently leads to a decreased initial level of AChE activity [103].

Regarding the liposome's formulations effect, the AChE activity is lower in the presence of liposomes with DODAP than without which may be partially explained by the increased stability of liposomes provided by the DODAP presence [101]. Overall, no significant difference between the values of AChE activity between the different liposomes concentrations was observed. Despite the high initial values of AChE activity in the cells incubated with the liposomes, as seen in Figures 21 to 24, a very significant decreasing tendency is observed within 50 minutes of reaction which may be indicative of an inhibition effect of the AChE activity thereafter. Thus, more and more prolonged replicates of this assay are required to further ascertain if the decreasing tendency is maintained. In addition, other complementary assays such as gene-silencing can be performed to determine if in fact liposomes possess inhibitory effect towards AChE.

5. Conclusion

The encapsulation of the curcumin and the siRNA in the liposomes had great results. All liposomes were performed with the ethanolic injection technique, and both the curcumin-loaded and siRNA-loaded liposomes did not become larger than 200 nm, which is the size limit that liposomes can have to being able to travel through the systemic circulation without clogging up capillaries. The formulations with DODAP, that is reported as a lipid that increases toxicity, were not more toxic to the cells than the formulations without DODAP plus the formulations with DODAP revealed a smaller size than the ones without DODAP. The siRNA-loaded liposomes, that can only be performed with DODAP to being able to encapsulate the siRNA due to the electrostatically interactions, presented a size of 150 nm. Using a mixture of curcumin-loaded liposomes with siRNA-loaded liposomes showed no differences relatively to the remaining formulations neither toxicity-wise nor in acetylcholinesterase activity values.

The MTT and PI/AO assays revealed similar results showing a dosage effect therefore proving that the lower concentrations of liposomes are less toxic to the cells. The encapsulation of curcumin and siRNA did not display any extra toxicity, which is a good sign since there is more possibilities to deliver these substances to the brain without further damage.

In the acetylcholinesterase activity assay, we verified that there is a significant downward trend in acetylcholinesterase activity in the cells incubated with the liposomes within 50 minutes of reaction, especially with the lower concentrations of liposomes. This leads to the conclusion that the lower concentration is both the less toxic (cell viability above 80%) and the one who may inhibit more the AChE activity. However, such inferences require further additional tests.

6. Future Work

Studies regarding the effect of liposomes in acetylcholinesterase activity and gene-silencing which were not possible to conclude in time are currently being performed.

Also, the next step is to test these liposomes formulations in zebrafish embryos, a reliable model for cytotoxicity and bioactivity assessment.

7. Bibliography

[1] N. Kulkarni e V. Bairagi, «Chapter One - Introduction», em *EEG-Based Diagnosis of Alzheimer Disease*, N. Kulkarni e V. Bairagi, Eds. Academic Press, 2018, pp. 1–24. doi: 10.1016/B978-0-12-815392-5.00001-0.

[2] A. M. Stewart *et al.*, «Molecular psychiatry of zebrafish», *Molecular Psychiatry*, vol. 20, n. 1, pp. 2–17, Fev. 2015, doi: 10.1038/mp.2014.128.

[3] S. Shams, J. Rihel, J. G. Ortiz, e R. Gerlai, «The zebrafish as a promising tool for modeling human brain disorders: A review based upon an IBNS Symposium», *Neuroscience & Biobehavioral Reviews*, vol. 85, pp. 176–190, Fev. 2018, doi: 10.1016/j.neubiorev.2017.09.002.

[4] T. Zhao, S. Zhang, Y. Guo, e Q. Wang, «TiC $_2$: a new two-dimensional sheet beyond MXenes», *Nanoscale*, vol. 8, n. 1, pp. 233–242, 2016, doi: 10.1039/C5NR04472C.

[5] Y.-H. Liao, Y.-J. Chang, Y. Yoshiike, Y.-C. Chang, e Y.-R. Chen, «Negatively Charged Gold Nanoparticles Inhibit Alzheimer's Amyloid-β Fibrillization, Induce Fibril Dissociation, and Mitigate Neurotoxicity», *Small*, vol. 8, n. 23, pp. 3631–3639, Dez. 2012, doi: 10.1002/smll.201201068.

[6] E. M. Caramillo e D. J. Echevarria, «Alzheimer's disease in the zebrafish: where can we take it?», *Behavioural Pharmacology*, vol. 28, pp. 179–186, Abr. 2017, doi: 10.1097/FBP.0000000000000284.

[7] C. A. Lane, J. Hardy, e J. M. Schott, «Alzheimer's disease», *European Journal of Neurology*, vol. 25, n. 1, pp. 59–70, Jan. 2018, doi: 10.1111/ene.13439.

[8] Alzheimer's Association, W. Thies, e L. Bleiler, «2013 Alzheimer's disease facts and figures», *Alzheimer's & Dementia*, vol. 9, n. 2, pp. 208–245, Mar. 2013, doi: 10.1016/j.jalz.2013.02.003.

[9] K. G. Yiannopoulou e S. G. Papageorgiou, «Current and future treatments for Alzheimer's disease», *Therapeutic Advances in Neurological Disorders*, p. 15, 2013.

[10] G. Tincer, «Neural stem/progenitor cells in Alzheimer's disease», p. 13, Mar. 2016.

[11] A. Stewart *et al.*, «The Developing Utility of Zebrafish in Modeling Neurobehavioral Disorders», p. 19, Jan. 2010.

[12] G. Šimić *et al.*, «Tau Protein Hyperphosphorylation and Aggregation in Alzheimer's Disease and Other Tauopathies, and Possible Neuroprotective Strategies», *Biomolecules*, vol. 6, n. 1, p. 6, Jan. 2016, doi: 10.3390/biom6010006.

[13] N. Gao, H. Sun, K. Dong, J. Ren, e X. Qu, «Gold-Nanoparticle-Based Multifunctional Amyloid-β Inhibitor against Alzheimer's Disease», *Chemistry - A European Journal*, vol. 21, n. 2, pp. 829–835, Jan. 2015, doi: 10.1002/chem.201404562.

[14] P. Taylor, S. Camp, e Z. Radić, «Acetylcholinesterase», em *Encyclopedia of Neuroscience*, L. R. Squire, Ed. Oxford: Academic Press, 2009, pp. 5–7. doi: 10.1016/B978-008045046-9.01132-3.

[15] P. Taylor e Z. Radić, «The cholinesterases: from genes to proteins», *Annu Rev Pharmacol Toxicol*, vol. 34, pp. 281–320, 1994, doi: 10.1146/annurev.pa.34.040194.001433.

[16] M. Jankowska, J. Wyszkowska, M. Stankiewicz, e J. Rogalska, «Molecular Targets for Components of Essential Oils in the Insect Nervous System-A Review», *Molecules*, vol. 23, Dez. 2017, doi: 10.3390/molecules23010034.

[17] L. O. Soto-Rojas *et al.*, «Neuroinflammation and Alteration of the Blood-Brain Barrier in Alzheimer´s Disease», em *Alzheimer's Disease - Challenges for the Future*, I. Zerr, Ed. InTech, 2015. doi: 10.5772/60024.

[18] G. Chen *et al.*, «Amyloid beta: structure, biology and structure-based therapeutic development», *Acta Pharmacol Sin*, vol. 38, n. 9, pp. 1205–1235, Set. 2017, doi:

10.1038/aps.2017.28.
[19] N. C. Wildburger *et al.*, «Amyloid-β Plaques in Clinical Alzheimer's Disease Brain Incorporate Stable Isotope Tracer In Vivo and Exhibit Nanoscale Heterogeneity», *Front. Neurol.*, vol. 9, p. 169, Mar. 2018, doi: 10.3389/fneur.2018.00169.
[20] P. I. Moreira *et al.*, «The Key Role of Oxidative Stress in Alzheimer's Disease», em *Oxidative Stress and Neurodegenerative Disorders*, Elsevier, 2007, pp. 267–281. doi: 10.1016/B978-044452809-4/50153-8.
[21] G. J. Burton e E. Jauniaux, «Oxidative stress», *Best Practice & Research Clinical Obstetrics & Gynaecology*, vol. 25, n. 3, pp. 287–299, Jun. 2011, doi: 10.1016/j.bpobgyn.2010.10.016.
[22] L. Martin, X. Latypova, e F. Terro, «Post-translational modifications of tau protein: Implications for Alzheimer's disease», *Neurochemistry International*, vol. 58, n. 4, pp. 458–471, Mar. 2011, doi: 10.1016/j.neuint.2010.12.023.
[23] J. C. Augustinack, A. Schneider, E.-M. Mandelkow, e B. T. Hyman, «Specific tau phosphorylation sites correlate with severity of neuronal cytopathology in Alzheimer's disease», *Acta Neuropathol*, vol. 103, n. 1, pp. 26–35, Jan. 2002, doi: 10.1007/s004010100423.
[24] H. Lee *et al.*, «Tau phosphorylation in Alzheimer's disease: pathogen or protector?», *Trends in Molecular Medicine*, vol. 11, n. 4, pp. 164–169, Abr. 2005, doi: 10.1016/j.molmed.2005.02.008.
[25] S. A. Youssef, «Pathology of Brain Aging and Animal Models of Neurodegenerative Diseases», em *Conn's Handbook of Models for Human Aging*, Elsevier, 2018, pp. 899–908. doi: 10.1016/B978-0-12-811353-0.00066-X.
[26] P. T. Nelson *et al.*, «Correlation of Alzheimer Disease Neuropathologic Changes With Cognitive Status: A Review of the Literature», *J Neuropathol Exp Neurol*, vol. 71, n. 5, pp. 362–381, Mai. 2012, doi: 10.1097/NEN.0b013e31825018f7.
[27] H. Sontheimer, «Aging, Dementia, and Alzheimer Disease», em *Diseases of the Nervous System*, Elsevier, 2015, pp. 99–131. doi: 10.1016/B978-0-12-800244-5.00004-5.
[28] K. H. Strang, T. E. Golde, e B. I. Giasson, «MAPT mutations, tauopathy, and mechanisms of neurodegeneration», *Laboratory Investigation*, vol. 99, n. 7, pp. 912–928, Jul. 2019, doi: 10.1038/s41374-019-0197-x.
[29] M. Tajes *et al.*, «The blood-brain barrier: Structure, function and therapeutic approaches to cross it», *Molecular Membrane Biology*, vol. 31, n. 5, pp. 152–167, Ago. 2014, doi: 10.3109/09687688.2014.937468.
[30] W. G. Mayhan, «Regulation of Blood–Brain Barrier Permeability», *Microcirculation*, vol. 8, n. 2, pp. 89–104, Mai. 2001, doi: 10.1038/sj.mn.7300154.
[31] R. Gabathuler, «Approaches to transport therapeutic drugs across the blood–brain barrier to treat brain diseases», *Neurobiology of Disease*, vol. 37, n. 1, pp. 48–57, Jan. 2010, doi: 10.1016/j.nbd.2009.07.028.
[32] S. Saif, A. Tahir, e Y. Chen, «Green Synthesis of Iron Nanoparticles and Their Environmental Applications and Implications», *Nanomaterials*, vol. 6, n. 11, p. 209, Nov. 2016, doi: 10.3390/nano6110209.
[33] M. Rafique, I. Sadaf, M. S. Rafique, e M. B. Tahir, «A review on green synthesis of silver nanoparticles and their applications», *Artificial Cells, Nanomedicine, and Biotechnology*, vol. 45, n. 7, pp. 1272–1291, Out. 2017, doi: 10.1080/21691401.2016.1241792.
[34] R. P. Feynman, «There's plenty of room at the bottom», *California Institute of Technology, Engineering and Science magazine*, 1960.
[35] M. Ovais *et al.*, «Green synthesis of silver nanoparticles via plant extracts: beginning a new era in cancer theranostics», *Nanomedicine*, vol. 11, n. 23, pp. 3157–3177, Dez. 2016, doi: 10.2217/nnm-2016-0279.

[36] V. Dhapte e V. Pokharkar, «Nanosystems for drug delivery: Design, engineering, and applications», em *Green Synthesis, Characterization and Applications of Nanoparticles*, Elsevier, 2019, pp. 321–345. doi: 10.1016/B978-0-08-102579-6.00013-7.
[37] C. Demetzos e N. Pippa, «Advanced drug delivery nanosystems (aDDnSs): a mini-review», *Drug Delivery*, vol. 21, n. 4, pp. 250–257, Jun. 2014, doi: 10.3109/10717544.2013.844745.
[38] P. Polak e O. Shefi, «Nanometric agents in the service of neuroscience: Manipulation of neuronal growth and activity using nanoparticles», *Nanomedicine: Nanotechnology, Biology and Medicine*, vol. 11, n. 6, pp. 1467–1479, Ago. 2015, doi: 10.1016/j.nano.2015.03.005.
[39] S. Kumar, V. Lather, e D. Pandita, «Green synthesis of therapeutic nanoparticles: an expanding horizon», *Nanomedicine*, vol. 10, n. 15, pp. 2451–2471, Ago. 2015, doi: 10.2217/nnm.15.112.
[40] H. Nadaroglu, A. A. Gungor, S. Ince, e A. Babagil, «Green synthesis and characterisation of platinum nanoparticles using quail egg yolk», *Spectrochimica Acta Part A: Molecular and Biomolecular Spectroscopy*, vol. 172, pp. 43–47, Fev. 2017, doi: 10.1016/j.saa.2016.05.023.
[41] M. Fernandes, I. Lopes, J. Teixeira, C. Botelho, e A. C. Gomes, «Exosome-Like Nanoparticles: A New Type Of Nanocarrier», *Current Medicinal Chemistry*, vol. 26, Jan. 2019, doi: 10.2174/0929867326666190129142604.
[42] J. Zhou, J. Ralston, R. Sedev, e D. A. Beattie, «Functionalized gold nanoparticles: Synthesis, structure and colloid stability», *Journal of Colloid and Interface Science*, vol. 331, n. 2, pp. 251–262, Mar. 2009, doi: 10.1016/j.jcis.2008.12.002.
[43] H. Jahangirian, E. Ghasemian lemraski, T. J. Webster, R. Rafiee-Moghaddam, e Y. Abdollahi, «A review of drug delivery systems based on nanotechnology and green chemistry: green nanomedicine», *International Journal of Nanomedicine*, vol. Volume 12, pp. 2957–2978, Abr. 2017, doi: 10.2147/IJN.S127683.
[44] K. N. Thakkar, S. S. Mhatre, e R. Y. Parikh, «Biological synthesis of metallic nanoparticles», *Nanomedicine: Nanotechnology, Biology and Medicine*, vol. 6, n. 2, pp. 257–262, Abr. 2010, doi: 10.1016/j.nano.2009.07.002.
[45] A. H. Tanzil, S. T. Sultana, S. R. Saunders, L. Shi, E. Marsili, e H. Beyenal, «Biological synthesis of nanoparticles in biofilms», *Enzyme and Microbial Technology*, vol. 95, pp. 4–12, Dez. 2016, doi: 10.1016/j.enzmictec.2016.07.015.
[46] J. Singh, T. Dutta, K.-H. Kim, M. Rawat, P. Samddar, e P. Kumar, «'Green' synthesis of metals and their oxide nanoparticles: applications for environmental remediation», *Journal of Nanobiotechnology*, vol. 16, n. 1, Dez. 2018, doi: 10.1186/s12951-018-0408-4.
[47] T. Borel e C. M. Sabliov, «Nanodelivery of Bioactive Components for Food Applications: Types of Delivery Systems, Properties, and Their Effect on ADME Profiles and Toxicity of Nanoparticles», *Annual Review of Food Science and Technology*, vol. 5, n. 1, pp. 197–213, Fev. 2014, doi: 10.1146/annurev-food-030713-092354.
[48] M. Rajabi e S. A. Mousa, «Lipid Nanoparticles and their Application in Nanomedicine», *Current Pharmaceutical Biotechnology*, vol. 17, n. 8, pp. 662–672, Mai. 2016, doi: 10.2174/1389201017666160415155457.
[49] R. Martín-Rapun, L. De Matteis, A. Ambrosone, S. Garcia-Embid, L. Gutierrez, e J. M. de la Fuente, «Targeted Nanoparticles for the Treatment of Alzheimer's Disease», *CPD*, vol. 23, n. 13, pp. 1927–1952, Mai. 2017, doi: 10.2174/1381612822666161226151011.
[50] C. He, Y. Hu, L. Yin, C. Tang, e C. Yin, «Effects of particle size and surface charge on cellular uptake and biodistribution of polymeric nanoparticles», p. 10, 2010.
[51] M. Agrawal *et al.*, «Recent advancements in liposomes targeting strategies to cross blood-brain barrier (BBB) for the treatment of Alzheimer's disease», *Journal of Controlled Release*, vol. 260, pp. 61–77, Ago. 2017, doi: 10.1016/j.jconrel.2017.05.019.

[52] L. Sercombe, T. Veerati, F. Moheimani, S. Y. Wu, A. K. Sood, e S. Hua, «Advances and Challenges of Liposome Assisted Drug Delivery», *Front. Pharmacol.*, vol. 6, Dez. 2015, doi: 10.3389/fphar.2015.00286.
[53] C. Ross, M. Taylor, N. Fullwood, e D. Allsop, «Liposome delivery systems for the treatment of Alzheimer’s disease», *IJN*, vol. Volume 13, pp. 8507–8522, Dez. 2018, doi: 10.2147/IJN.S183117.
[54] K. Wong *et al.*, «Review of Current Strategies for Delivering Alzheimer's Disease Drugs across the Blood-Brain Barrier», *IJMS*, vol. 20, n. 2, p. 381, Jan. 2019, doi: 10.3390/ijms20020381.
[55] E. van der Pol, A. Böing, P. Harrison, A. Sturk, e R. Nieuwland, «Classification, Functions, and Clinical Relevance of Extracellular Vesicles», *Pharmacological reviews*, vol. 64, pp. 676–705, Jun. 2012, doi: 10.1124/pr.112.005983.
[56] X. Li *et al.*, «Challenges and opportunities in exosome research-Perspectives from biology, engineering, and cancer therapy», *APL Bioeng*, vol. 3, n. 1, pp. 011503–011503, Mar. 2019, doi: 10.1063/1.5087122.
[57] M. Lin e X.-R. Qi, «Purification Method of Drug-Loaded Liposome», em *VDI-Wärmeatlas*, P. Stephan, D. Mewes, S. Kabelac, M. Kind, K. Schaber, e T. Wetzel, Eds. Berlin, Heidelberg: Springer Berlin Heidelberg, 2019, pp. 1–11. doi: 10.1007/978-3-662-49231-4_24-1.
[58] G. A. Reineccius, «Liposomes for Controlled Release in the Food Industry», em *Encapsulation and Controlled Release of Food Ingredients*, vol. 590, S. J. Risch e G. A. Reineccius, Eds. Washington, DC: American Chemical Society, 1995, pp. 113–131. doi: 10.1021/bk-1995-0590.ch011.
[59] S. Vemuri e C. T. Rhodes, «Preparation and characterization of liposomes as therapeutic delivery systems: a review», *Pharmaceutica Acta Helvetiae*, vol. 70, n. 2, pp. 95–111, Jul. 1995, doi: 10.1016/0031-6865(95)00010-7.
[60] O. K. Nag e V. Awasthi, «Surface engineering of liposomes for stealth behavior», *Pharmaceutics*, vol. 5, n. 4, pp. 542–569, Out. 2013, doi: 10.3390/pharmaceutics5040542.
[61] A. Gabizon e D. Papahadjopoulos, «Liposome formulations with prolonged circulation time in blood and enhanced uptake by tumors», *Proc Natl Acad Sci U S A*, vol. 85, n. 18, pp. 6949–6953, Set. 1988, doi: 10.1073/pnas.85.18.6949.
[62] J. L. Hood, «Post isolation modification of exosomes for nanomedicine applications», *Nanomedicine*, vol. 11, n. 13, pp. 1745–1756, Jul. 2016, doi: 10.2217/nnm-2016-0102.
[63] D. Vieira e L. Gamarra, «Getting into the brain: liposome-based strategies for effective drug delivery across the blood–brain barrier», *IJN*, vol. Volume 11, pp. 5381–5414, Out. 2016, doi: 10.2147/IJN.S117210.
[64] V. Tello-Franco, M. Lozada-Garcia, e M. Soriano-Garcia, «Experimental and Computational Studies on the Inhibition of Acetylcholinesterase by Curcumin and Some of its Derivatives», *CAD*, vol. 9, n. 2, pp. 289–298, Jun. 2013, doi: 10.2174/15734099113099990007.
[65] M. Hasan *et al.*, «Liposome encapsulation of curcumin: Physico-chemical characterizations and effects on MCF7 cancer cell proliferation», *International Journal of Pharmaceutics*, vol. 461, n. 1–2, pp. 519–528, Jan. 2014, doi: 10.1016/j.ijpharm.2013.12.007.
[66] H. Dana *et al.*, «Molecular Mechanisms and Biological Functions of siRNA», vol. 13, n. 2, p. 10, 2017.
[67] A. A. Mokhtarieh, J. Lee, S. Kim, e M. K. Lee, «Preparation of siRNA encapsulated nanoliposomes suitable for siRNA delivery by simply discontinuous mixing», *Biochimica et Biophysica Acta (BBA) - Biomembranes*, vol. 1860, n. 6, pp. 1318–1325, Jun. 2018, doi: 10.1016/j.bbamem.2018.02.027.
[68] Y. Xia, J. Tian, e X. Chen, «Effect of surface properties on liposomal siRNA delivery»,

Biomaterials, vol. 79, pp. 56–68, Fev. 2016, doi: 10.1016/j.biomaterials.2015.11.056.
[69] D. Clarke, A. Idris, e N. A. J. McMillan, «Development of novel lipidic particles for siRNA delivery that are highly effective after 12 months storage», p. 8, 2019.
[70] A. C. N. Oliveira, J. Fernandes, A. Gonçalves, A. C. Gomes, e M. E. C. D. R. Oliveira, «Lipid-based Nanocarriers for siRNA Delivery: Challenges, Strategies and the Lessons Learned from the DODAX: MO Liposomal System», *CDT*, vol. 20, n. 1, pp. 29–50, Nov. 2018, doi: 10.2174/1389450119666180703145410.
[71] A. Schroeder, C. G. Levins, C. Cortez, R. Langer, e D. G. Anderson, «Lipid-based nanotherapeutics for siRNA delivery», p. 13, 2010.
[72] A. Santel *et al.*, «A novel siRNA-lipoplex technology for RNA interference in the mouse vascular endothelium», *Gene Ther*, vol. 13, n. 16, pp. 1222–1234, Ago. 2006, doi: 10.1038/sj.gt.3302777.
[73] T. P. Herringson, R. R. Patlolla, e J. G. Altin, «Targeting of plasmid DNA-lipoplexes to cells with molecules anchored via a metal chelator lipid», *J. Gene Med.*, vol. 11, n. 11, pp. 1048–1063, Nov. 2009, doi: 10.1002/jgm.1394.
[74] P. Vader, L. J. van der Aa, J. F. J. Engbersen, G. Storm, e R. M. Schiffelers, «A method for quantifying cellular uptake of fluorescently labeled siRNA», *Journal of Controlled Release*, vol. 148, n. 1, pp. 106–109, Nov. 2010, doi: 10.1016/j.jconrel.2010.06.019.
[75] L. Y. Rizzo *et al.*, «In vivo nanotoxicity testing using the zebrafish embryo assay», *J. Mater. Chem. B*, vol. 1, n. 32, pp. 3918–3925, 2013, doi: 10.1039/C3TB20528B.
[76] R. Gerlai, «Using zebrafish to unravel the genetics of complex brain disorders», em *Behavioral neurogenetics*, Springer, 2011, pp. 3–24.
[77] M. Grit e D. J. A. Crommelin, «Chemical stability of liposomes: implications for their physical stability», *Chemistry and Physics of Lipids*, vol. 64, n. 1–3, pp. 3–18, Set. 1993, doi: 10.1016/0009-3084(93)90053-6.
[78] S. Bhattacharjee, «DLS and zeta potential – What they are and what they are not?», *Journal of Controlled Release*, vol. 235, pp. 337–351, Ago. 2016, doi: 10.1016/j.jconrel.2016.06.017.
[79] R. A. Nixon, «Endosome function and dysfunction in Alzheimer's disease and other neurodegenerative diseases», *Neurobiology of Aging*, vol. 26, n. 3, pp. 373–382, Mar. 2005, doi: 10.1016/j.neurobiolaging.2004.09.018.
[80] M. D. Ard, G. M. Cole, J. Wei, A. P. Mehrle, e J. D. Fratkin, «Scavenging of Alzheimer's Amyloid P-Protein by Microglia in Culture», p. 13, 1996.
[81] E. Forssen e M. Willis, «Ligand-targeted liposomes», *Advanced Drug Delivery Reviews*, p. 23, 1998.
[82] S. M. Moghimi e J. Szebeni, «Stealth liposomes and long circulating nanoparticles: critical issues in pharmacokinetics, opsonization and protein-binding properties», *Progress in Lipid Research*, vol. 42, n. 6, pp. 463–478, Nov. 2003, doi: 10.1016/S0163-7827(03)00033-X.
[83] K. G. Ozdemir, H. Yılmaz, e S. Yılmaz, «In vitro evaluation of cytotoxicity of soft lining materials on L929 cells by MTT assay», *J. Biomed. Mater. Res.*, vol. 90B, n. 1, pp. 82–86, Nov. 2008, doi: 10.1002/jbm.b.31256.
[84] J. Kovalevich e D. Langford, «Considerations for the Use of SH-SY5Y Neuroblastoma Cells in Neurobiology», p. 13, 2013.
[85] Y. T. Mak, W. P. Lam, L. Lü, Y. W. Wong, e D. T. Yew, «The toxic effect of ketamine on SH-SY5Y neuroblastoma cell line and human neuron», *Microscopy Research and Technique*, vol. 73, n. 3, pp. 195–201, Mar. 2010, doi: 10.1002/jemt.20774.
[86] M. J. Stoddart, Ed., *Mammalian Cell Viability*, vol. 740. Totowa, NJ: Humana Press, 2011. doi: 10.1007/978-1-61779-108-6.
[87] W. Strober, «Trypan Blue Exclusion Test of Cell Viability», *Current Protocols in Immunology*,

vol. 111, n. 1, Nov. 2015, doi: 10.1002/0471142735.ima03bs111.
[88] A. Yip, D. K. N. e N. Auersperg, «The dye-exclusion test for cell viability: Persistence of differential staining following fixation», p. 7, 1972.
[89] J. M. Capasso, B. R. Cossío, T. Berl, C. J. Rivard, e C. Jiménez, «A colorimetric assay for determination of cell viability in algal cultures», *Biomolecular Engineering*, vol. 20, n. 4–6, pp. 133–138, Jul. 2003, doi: 10.1016/S1389-0344(03)00037-6.
[90] K. Präbst, H. Engelhardt, S. Ringgeler, e H. Hübner, «Basic Colorimetric Proliferation Assays: MTT, WST, and Resazurin», p. 17, 2017.
[91] V. A. Byvaltsev *et al.*, «Acridine Orange: A Review of Novel Applications for Surgical Cancer Imaging and Therapy», *Front. Oncol.*, vol. 9, p. 925, Set. 2019, doi: 10.3389/fonc.2019.00925.
[92] Ö. S. Aslantürk, «In Vitro Cytotoxicity and Cell Viability Assays: Principles, Advantages, and Disadvantages», em *Genotoxicity - A Predictable Risk to Our Actual World*, M. L. Larramendy e S. Soloneski, Eds. InTech, 2018. doi: 10.5772/intechopen.71923.
[93] S. Kamiloglu, G. Sari, T. Ozdal, e E. Capanoglu, «Guidelines for cell viability assays», p. 18, 2020.
[94] Ö. S. Aslantürk, «In Vitro Cytotoxicity and Cell Viability Assays: Principles, Advantages, and Disadvantages», em *Genotoxicity - A Predictable Risk to Our Actual World*, M. L. Larramendy e S. Soloneski, Eds. InTech, 2018. doi: 10.5772/intechopen.71923.
[95] C. Cheng, S. Peng, Z. Li, L. Zou, W. Liu, e C. Liu, «Improved bioavailability of curcumin in liposomes prepared using a pH-driven, organic solvent-free, easily scalable process», *RSC Adv.*, vol. 7, n. 42, pp. 25978–25986, 2017, doi: 10.1039/C7RA02861J.
[96] A. A. Mokhtarieh, «Preparation of siRNA encapsulated nanoliposomes suitable for siRNA delivery by simply discontinuous mixing», p. 8, 2018.
[97] F. Haghiralsadat, G. Amoabediny, S. Naderinezhad, T. Forouzanfar, M. N. Helder, e B. Zandieh-Doulabi, «Preparation of PEGylated cationic nanoliposome-siRNA complexes for cancer therapy», *Artificial Cells, Nanomedicine, and Biotechnology*, vol. 46, n. sup1, pp. 684–692, Out. 2018, doi: 10.1080/21691401.2018.1434533.
[98] S. Cui *et al.*, «Correlation of the cytotoxic effects of cationic lipids with their headgroups», *Toxicology Research*, vol. 7, n. 3, pp. 473–479, Mai. 2018, doi: 10.1039/c8tx00005k.
[99] A. Jaszczyszyn e K. Gąsiorowski, «Limitations of the MTT Assay in Cell Viability Testing», p. 5, 2008.
[100] L. Gutiérrez *et al.*, «1.09 - Nanotechnology in Drug Discovery and Development», em *Comprehensive Medicinal Chemistry III*, S. Chackalamannil, D. Rotella, e S. E. Ward, Eds. Oxford: Elsevier, 2017, pp. 264–295. doi: 10.1016/B978-0-12-409547-2.12292-9.
[101] M. Fernandes *et al.*, «Novel concept of exosome-like liposomes for the treatment of Alzheimer's disease», *Journal of Controlled Release*, vol. 336, pp. 130–143, Ago. 2021, doi: 10.1016/j.jconrel.2021.06.018.
[102] M.-S. García-Ayllón, D. H. Small, J. Avila, e J. Sáez-Valero, «Revisiting the role of acetylcholinesterase in Alzheimer's disease: cross-talk with P-tau and β-amyloid», *Frontiers in Molecular Neuroscience*, p. 9, 2011.
[103] W. Sun *et al.*, «Study of acetylcholinesterase activity and apoptosis in SH-SY5Y cells and mice exposed to ethanol», *Toxicology*, vol. 384, pp. 33–39, Jun. 2017, doi: 10.1016/j.tox.2017.04.007.